PEOPLE'S DEMOCRATIC REPUBLIC OF ALGERIA
Ministry of Higher Education and Scientific Research
University of Kasdi Merbah Ouargla
Faculty of Mathematics and Matter Sciences
Department of Chemistry

MASTER'S THESIS

Specialization: Materials Chemistry

Presented by:
Ranya BELAHBIB & Fatima BENLAID

Preparation of Polyurethane Foams from Castor Oil Bio-sourced Polyols

Board of Examiners:

Full Name	Rank / Role	Institution
Pr. **Moussaoui Yacine**	Supervisor	UKM Ouargla
Pr. **Zeghdi Saad**	Co-Supervisor	UHL El Oued
Pr. **Zenkhri Louiza**	President	UKM Ouargla
Pr. **Zaoui Manel**	Examiner	UKM Ouargla

Publicly discussed on: June 14, 2026

Academic Year: 2025/2026

PEOPLE'S DEMOCRATIC REPUBLIC OF ALGERIA
Ministry of Higher Education and Scientific Research
University of Kasdi Merbah Ouargla
Faculty of Mathematics and Matter Sciences
Department of Chemistry

MASTER'S THESIS

Specialization: Materials Chemistry

Presented by:
Ranya BELAHBIB & Fatima BENLAID

Preparation of Polyurethane Foams from Castor Oil Bio-sourced Polyols

Board of Examiners:

Full Name	Rank / Role	Institution
Pr. **Moussaoui Yacine**	Supervisor	UKM Ouargla
Pr. **Zeghdi Saad**	Co-Supervisor	UHL El Oued
Pr. **Zenkhri Louiza**	President	UKM Ouargla
Pr. **Zaoui Manel**	Examiner	UKM Ouargla

Publicly discussed on: June 14, 2026

Academic Year: 2025/2026

DEDICATION

إلى نفسي...

إلى تلك التي خاضت الطريق بكل ما فيه من تعبٍ وتحدّي، إلى روحي التي تعبت ولم تتكسر، وسقطت ولم استسلت، إلى قلبي

الذي آمن أن الالأحلاك لالا تُبدى بل تُنتزع بالصبر، أهديكِ هذا النجاح لالأنكِ كنتِ داكمًا على قدر الحلت والمسؤوليةc إلى أبي الغالي خمد الالأمين...

إلى سندي الذي لالا يميل، إلى من كان يتفقد نومه ليوقظني و يُوصلني إلى الحافلة باكرًا، إلى من اختار تعبي على تعبه وراحتي على

راحته، لكَ هذا الالإنجاز عبيون وفاءٍ وحبٍّ لالا ينتويc إلى أحي

الحبيبة مسعودي أمال...

يا قلبًا احتواني قبل أن أعبف معنى الحياة، يا دعوةً صادقة كانت ترافقني في كل خطوة، يا دفئًا 2يميني ونورًا مبديني، هذا

التخرج ثمرة تعبكِ وصبركِ ودعواتكِ التي صنعت لي الطريقc إلى إخوتي فرسان

وعاائشة...

أنتم نبض الفرح في حياتي، بكم مبون الطريق وتكبر الالابتسامةc إلى خطيبي الورقلي

نورالدين...

إلى من كان قوةً حين ضعفت، وأملًاك حين تعبت، شكرًا لدعمك الذي لم ينقطع، وجودك في حياتي طمأنينة أعتز بباc إلى عائلتي الكريمة مسعودي

وبالحبيب...

أنتم الالأصل الذي أن تي إليه بفخر، ومنكم أس هد العزيمة والثباتc إلى إخوتي شاهين

وشامل...

يا من 22معني ب6م| راب& الدم والروح، وجود/م| في حياتي نعمة وسندc إلى صديقتي

الالأكثر من أخت دعاء فراجي...

يا من كانت بقربي في كل التفاصيل، كنتِ داكمًا أقرب مما يُقالc

الى رفيقة الدرب واجمل الصدف عاائشة عبباوي ،اهديك عملي تقديرا مح7بتك و دعمك إلى أخواتي من

صلب العائلة شكران بالحبيب , هاجرعماري, إكرام شاشة، هبة بالحبيب ...

بكنّ تحلو اللقاءات وترهر الالأيامc

إلى ريكاتي في السكن الجامعي فاطمةقوال ، هدى قبي ،نور ,حليمة ...

رفيقات السبر والتعب والضحكات، كنق ُ ّن عائلتي الثانية في أجمل وأصعب المراحلc إلى أشخاص لقيتني بيم

الحياة صدفة،

فكانوا أقوى سند وأصدق دعم، وجوددم لم يكن عايزًا، بل كان أثرًا طيبًا لالا يُنسىc إليكم جميعًا أهدي ثمرة

سنواتٍ من السبر والتعب والصبر،

أهديكم حSًا كبر معي حتى أصبح حقيقة، فأنتم بعد اكاللهلله النور الذي أضاء طريقي، والقوة التي دفعتني للأ مام، هذا التخرج ليس

إنجازي وحدي، بل هو نجاحٌ 2يمل أسماءدم في قلبي قبل أن يُكتب باسميc

أسأل اكاللهلله أن يجزيكم عني خير الجزاء، وأن يجعل فرحتي هذه بداية أفراح أكبر ت2معنا داكمًاc

رانيا بالحبيب

"من قال أنا لها نالها... وأنا لها، وان استعصت يومًا أتيتُ بيا ر"مًا عن كل الصعابc" الى نفسي cccc

لم تكن الرحلة قصيرة، ولم يكن الطريق مفروشًا باليسر، ولم يكن الحلت قريب المنال... لكنه كان يسكنني، يؤرقني، ويوقظ فيّ روح التحدي كلما تعثّرتc

سعيت، صبرت، تعبت، وبكيت أحيانًا... لكنني لم أستسلتc

واليوم أقف شاعخة بما حققته، لالأنني آمنت أن من يررع الالإصرار يحصد النجاحc نعم... فعلتبا ونلتبا إلى الذي زينّ اسمي بأجمل الالألقاب، من دعمني بلاك حدود وأعطاني بلاك مقابل...

من عّSمني أن الدنيا كفاح وسلاكحه العلت والمعرفة، وكان سندي وقوتي وملاكذي بعد االلهله... إلى عفري واعتزازي، أبي خممدc

إلى من جعل االلهله الجنة تحت أقدامبا، فاحتضنتني قلبًا قبل يدمبا، وسبّلت لي الشدائد بدعائبا...

إلى القلب الحنون والشمعة التي أضاءت لي الليالي المظSمات، سرّ قوتي ونجاحي وداعمي الالأول في مسيرتي... إلى أحي لعقاب مبيمc

إلى ضلعي الثابت وأمان أياحي، إلى من شددت عضدي بيم فكانوا لي ينابيع أرتوي منبا، إلى خبرة أياحي وصدقها، إلى قرة عيني... إلى إخوتي عبلة وحفيظة، إيراهم ونبيل وحسينc

إلى من أفاضني بمشاعبه ونصائحه امج لصة، وكان بصمة نور في طريقي... إلى صديق العمر قبل أن يكون خالي... قويدرc

لكل من كان عونًا وسندًا في هذا الطريق... للأ صدقاء الالأوفياء، ورفقاء السنين، وأححاب الشدائد والالأزمات... إلى رفيقة الدرب... صونيا بن جدوc

هذا ليس عجرد إنجاز يُكتب، بل قصة كفاح تُروى، وحلت طال انتظاره حتى صار حقيقة بين يديّc

ها أنا اليوم أقطف أولى ثمار تعبي، وأعلن بفخر أن ما كان يومًا أمنية أصبح واقعًا بفضل االلهله ثم بدعمكمc اللهم لك امحمد حتى يبلغ امحمد منتباه، ولك امحمد إذا رضيت، ولك امحمد بعد الرضاc

H-من سار على الدرب وصل... وأنا وصلت، وبإذن االلهله ما زال في الطريق نجاحات أكبر وأحلالم أعظم تنتظرنيc

بن العيد فطيمة

ACKNOWLEDGMENT

نتقدم بأسمى عبارات الشكر والتقدير والامتنان إلى الأستاذ المشرف الأستاذ ، موساوي ياسين
الذي كان لنا خير موجّه وداعم طوال مسيرة إنجاز هذه المذكرة، فبصبره، وتفانيه، وتوجيهاته القيّمة، أضاء لنا طريق البحث،
وكان لف برته ونصائحه الأثر الكبير في إخراج هذا العمل بأفضل صورة ممكنةc فله منا كل الاحترام والعرفان، وأسأل اللهالله أن يجز يه عنا خير الجزاء وأن يوفقه لمزيد من التألق والعطاء العSميc

/م نتقدم بخالص الشكر والتقدير إلى رئيسة قسم الكيمياء الأستاذة ، زنخري لويرة
التي كانت لنا بمثابة الأم، بما قدمته لنا من دعم واهتمام واشجيع دائم، فكانت كلماتبا ومساندتبا دافعًا لنا للأكس هرار والاجتباد،
فلها منا أصدق عبارات الامتنان وامج7بةc

/م نتوجه بجز يل الشكر إ لعسؤول الأرضية التقنية لتحاليل الفيز يو كيميائية CRAPC الدكتور بوخالفة عبد الحكيم خاصة، والى جميع طاقم الأرضية عامة، على حسن الاستقبال والتعاون والتسبيلاك المقدمة لنا طيلة فترة العملc

ولا يفوتنا أن نعبر عن خالص امتناننا إلى ركة رغوة الجنوب تقرت بصفة عامة، والى السيد طلبية بصفة خاصة، على دعمهم ومبافقتبم القيمة، التي كان لها دور كبير في إنجاح هذا العملc

فإلى كل من ساهم من قريب أو بعيد في إنجاز هذه المذكرة، نتقدم بأصدق عبارات الشكر والتقديرc

ABSTRACT

This study demonstrates the viability of utilizing castor oil as a renewable, bio-sourced alternative to synthetic polyol (polypropylene glycol - PPG) in the production of polyurethane foams (PUFs). Three distinct foam formulations were developed and analyzed to control the open-to-closed cell ratio: a pure synthetic foam (PU1 - 100% PPG), a hybrid blend (PU2 - Castor Oil + PPG), and a pure bio-based foam (PU3 - 100% Castor Oil). The structural, physical, and morphological properties were comprehensively evaluated using Fourier-Transform Infrared Spectroscopy (FTIR) and Scanning Electron Microscopy coupled with Energy Dispersive X-ray Spectroscopy (SEM-EDX). The characterization results revealed that the hybrid blend (PU2) exhibited the highest density and the lowest water absorption, making it highly suitable for rigid insulation applications. Conversely, the pure synthetic foam (PU1) exhibited a highly porous network with the highest water absorption (913%), rendering it ideal for filtration and absorption systems. Ultimately, these outcomes confirm that castor oil represents an effective sustainable precursor for tailoring the performance of eco-friendly polyurethane foams tailored for specific industrial needs.

Keywords: Polyurethane Foam (PUF), Bio-sourced Polyols, Castor Oil, SEM/EDX, Water Absorption.

ملخص المذكرة

تتناول هذه الدراسة تقيهم إمكانية استخدام زيت الفروع كبديل حيوي ومستدام للبوليول الالاصطناعي (PPG) في إنتاج رغوة البولي يوريثان c(PUFs) تم تحضير ودراسة ثلاث تركيبات عختلفة للرغوة للتحكم في بنية الفلاكيا المفتوحة والمغلقة: التركيبة

الالأولى اعتمدت بالكامل على البوليول الالاصطناعي (100% ،(PPG التركيبة الثانية شكلت مزيجاً جيناً (زيت الفروع + ،PPG

(بينما اعتمدت التركيبة الثالثة بالكامل على البوليول الحيوي (100% زيت الفروع)c أظهرت نتائج التوصيف الفيز ياني والـكيمياني والميكانيكي بواسطة مطيافية الالأشعة تحت امcراء ،(FTIR) وامحجهر الالإلـكتروني الما # (SEM-EDK) تمكّن الدراسة من ضب&

الفصائص بدقة؛ حيث تميز المز ج الهجين (PU2) بأعلى ث افة وأقل قدرة على امتصاص الماء، مما يجعله مثالياً لتطبيقات العزل

الصلبc في المقابل، لجلت الرغوة الالاصطناعية (PU1) أعلى آسبة امتصاص لـ3ماء بنسبة (91S%) نظراً لبنيتبا المسامية المفتوحة المترابطة, مما يرشحها لالأنظمة الترشيح والالامتصاصc وتؤكد هذه النتائج نجاح استخدام زيت الفروع كمصدر متجدد لالإنتاج مواد بولي يوريثان صديقة للبيئة وذات خصائص قابلة للتعديل حسب التطبيقات الصناعيةc

الكلمات المفتاحية: رغوة البولي يوريثان ،(PUF) بوليولالات حيوية المصدر، زيت الفروع، البنية المورفولوجية ،(SEM/EDK) امتصاص الماءc

Cette étude démontre la viabilité de l'utilisation de l'huile de ricin comme alternative biosourcée et renouvelable au polyol synthétique (polypropylène glycol - PPG) pour la production de mousses de polyuréthane (PUFs). Trois formulations distinctes ont été élaborées afin de contrôler précisément le rapport entre cellules ouvertes et fermées : une mousse purement synthétique (PU1 - 100% PPG), un mélange hybride (PU2 - Huile de ricin + PPG), et une mousse purement biosourcée (PU3 - 100% Huile de ricin). Les caractérisations physico-chimiques, morphologiques et mécaniques ont été menées par spectroscopie infrarouge à transformée de Fourier (FTIR) et par microscopie électronique à balayage (MEB-EDX). Les résultats indiquent que le mélange hybride (PU2) présente la densité la plus élevée et l'absorption d'eau la plus faible, ce qui le rend idéal pour les applications d'isolation rigide. À l'inverse, la mousse synthétique (PU1) se distingue par un réseau hautement poreux avec une absorption d'eau maximale (913%), propice aux systèmes de filtration et d'absorption. En conclusion, ces travaux confirment le potentiel de l'huile de ricin en tant que précurseur durable pour la conception de mousses polyuréthanes écologiques aux propriétés ajustables selon les exigences industrielles.

Mots-clés : Mousse de Polyuréthane (PUF), Polyols Biosourcés, Huile de Ricin, MEB/EDX, Absorption d'eau.

Contents

List of Figures

List of Tables

GENERAL INTRODUCTION

Plastics have fundamentally reshaped modern manufacturing due to their versatility and advantageous properties. As synthetic polymers, they are lightweight, durable, waterproof, moldable, and cost-effective, making them superior substitutes for traditional materials like wood and metals across numerous sectors [5] . This has led to their widespread adoption in packaging, automotive, aerospace, construction, electronics, healthcare, and consumer goods, where replacing metal parts with lightweight polymers notably improves fuel efficiency in vehicles and electric vehicles [[5]]. The global market for plastics was valued at over USD 545 billion in 2025, and global production is estimated at around 430 to 446 million tonne. Production has seen consistent growth, rising 4.1% in 2024 compared to the previous year, although with significant regional disparities, as Asia, particularly China, now accounts for over 57% of global output, highlighting the material's central role in the modern global economy [6].

Polyurethanes (PUs) are a class of polymers produced via condensation polymerization reactions between polyols and diisocyanates. These versatile materials can be tailored into various forms, including rigid and flexible foams, elastomers, coatings, adhesives, and fibers [[7]]. This tenability makes them indispensable in numerous industries such as construction for insulation, automotive for light weighting, furniture for cushioning, and the medical and electronics sectors for specialty applications. The global polyurethane market was estimated at roughly USD 87-90 billion in 2025 and is projected to grow significantly in the coming years [8]. The increasing demand for sustainable products is a major trend, driving innovation in developing bio-based polyurethanes derived from renewable sources. As global production is expected to reach 22.5 million tons, the synthesis and application of polyurethanes remain a vibrant field of materials science [7].

The environmental persistence of conventional plastics has made recycling a crucial element of waste management and the transition to a circular green economy. Traditional recycling methods face substantial challenges, including high costs and the non-recyclability of certain materials, which hinder broader application [9]. As a result, a significant shift is underway towards more sustainable and recyclable polymers, promoting a circular economy. Key to this transition are next-generation biodegradable polymers, which are emerging as promising alternatives to petrochemical plastics [10]. The integration of these biodegradable bioplastics in biorefineries offers a pathway for cost reduction and low waste generation, aligning with circular bioeconomy principles. This approach is essential as global plastic waste accumulates, with over 400 million tons produced annually and a vast majority being improperly discarded [9].

The search for environmentally friendly polymers has spurred extensive research into the preparation of polyurethanes from biodegradable polyols. A promising route involves valorizing waste biomass, where corn cob lignocellulosic waste can be transformed via microwave-assisted depolymerization into a bio-based polyol for producing rigid polyurethane foams. Other successful

syntheses have utilized bio-polyols derived from sources such as olive seed oil, lignin from wood, and even oligosaccharides like raffinose, which can be reacted with toluene diisocyanate (TDI) to produce polyurethanes. This approach not only enables the creation of polyurethane materials that exhibit excellent thermal and mechanical robustness but also promotes waste valorization. By incorporating bio-based and biodegradable polyols, it becomes possible to develop next-generation polyurethanes with a significantly reduced environmentalfootpri[11–14].

The present study focuses on the synthesis and characterization of novel polyurethane materials derived from bio-sourced polyols. The objective is to formulate sustainable polyurethanes by reacting these renewable polyols with toluene diisocyanate (TDI), one of the most dominant aromatic diisocyanates used in polyurethane chemistry. Various synthesis routes will be explored to prepare the polyurethanes, drawing from established procedures for bio-based polyurethane production, such as the one-shot method. The resulting polymers will be characterized using analytical techniques like FTIR to confirm their structure and to evaluate how the nature of the bio-polyol influences thermal stability and mechanical properties. This investigation aims to contribute to the growing field of eco-friendly materials, offering an alternative to conventional petrochemical-based polyurethanes.

Chapter I

LITERATURE REVIEW

I.1 Overview of Polyurethanes (PU)

From a materials science perspective, Polyurethanes are segmented block copolymers. They consist of alternating sequences of flexible, low glass transition temperature (T_g) "soft segments" (polyols) and rigid, high T_g "hard segments" (isocyanates and chain extenders). This phase-separated morphology is what gives PU its unique mechanical properties...?? Polyurethanes, commonly abbreviated as

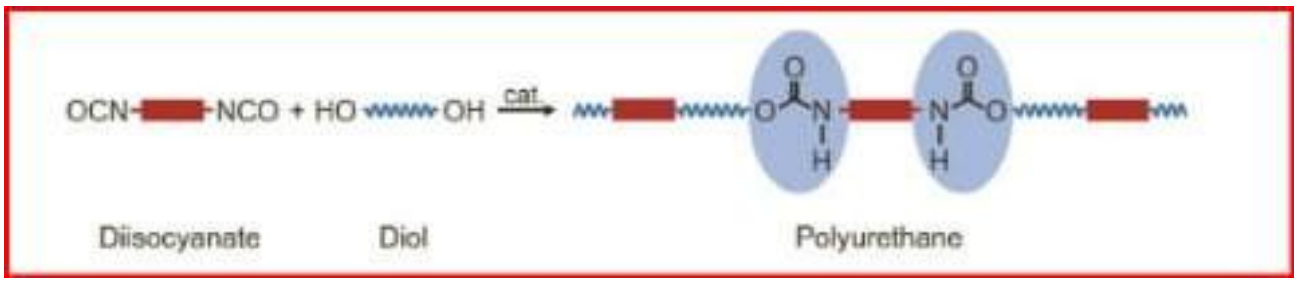

Figure I.1: Polyaddition reaction of a diisocyanate and a diol to form a polyurethane.

PUR and also referred to as urethanes, represent a diverse class of materials with a wide range of applications. Their structure is defined by the urethane linkage (-NH- C(=O)- O-). This class of polymers was first discovered in 1937 by Otto Von Bayer and his colleagues.
Polyurethanes can be classified as esters or amide esters of carbonic acid. They are produced through the reaction between polyfunctional hydroxyl compounds and polyfunctional isocyanates.[15]

I.2 Polyurethanes Synthesis process

I.2.1 Polyurethanes Synthesis method

PU synthesis method has a one-step synthesis process and two-step synthesis process. Although the two methods are diff erent, the chemical principle behind both methods is similar.

One step Synthesis process

The one-step synthesis process involves combining all polyurethane raw materials—such as isocyanate, polyol, and chain extender—in a single reaction mixture. In this approach, the reaction between iso-

cyanate and polyol, as well as the subsequent reaction of the resulting prepolymer with the chain extender, occur simultaneously.

Two step Synthesis process

The two-step process involves reacting the polyol with the polyisocyanate first to produce a prepolymer of sufficient molecular weight. Subsequently, a chain extender is added to the resulting prepolymer to transform it into a high-molecular-weight compound.

The prepolymer produced by the initial reaction of polyols and polyisocyanates is inherently soft and possesses very low mechanical strength. Therefore, a chain extender must be added to form a polymer that has practical utility. While the prepolymer can be sold as a standalone product, certain additives are often required to extend its shelf life.

Although polyurethane synthesis can be conducted via two different methods, the underlying principles remain similar; the primary difference lies in the sequence of addition. However, most experts suggest that the two-step method is generally superior to the one-step system, as it results in higher product quality.[16]

I.3 Polyurethane Foaming Systems

Foaming systems are categorized into three types based on the chemicals used in the synthesis process:

- One-step one-shot system
- Quasi-prepolymer system
- Full prepolymer system

Among these, the one-step and quasi-prepolymer systems are the most commonly used in the foaming industry. The one-step process is the predominant method, whereas prepolymer systems were primarily used in the early days of the urethane industry. In the one-step system, Component A and Component B are kept separate. Component A consists solely of polyisocyanate, while Component B contains polyol, surfactant, blowing agent, and catalyst. When the two components are mixed, foam is formed.

In a quasi-prepolymer system, Component A consists of a polyisocyanate combined with a portion of the polyol, while Component B contains the remaining polyol along with the rest of the formulation ingredients, such as catalyst and blowing agent. The foaming product is formed upon mixing the two components.

In a full prepolymer system, Component A is composed of polyisocyanate combined with polyol. Component B contains no polyol; instead, it includes the remaining formulation ingredients such as blowing agents, surfactants, and catalysts. The reaction is initiated when Components A and B are mixed.

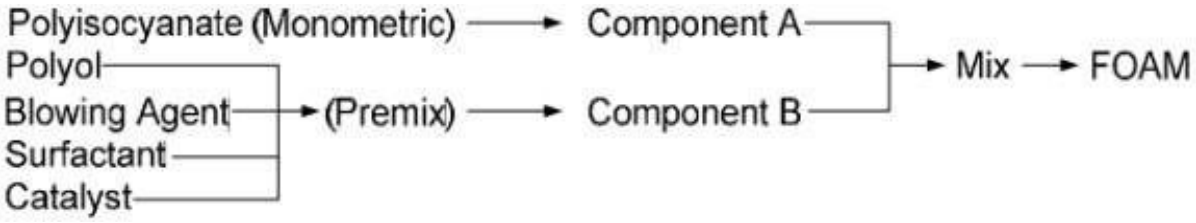

Figure I.2: One step one shot system

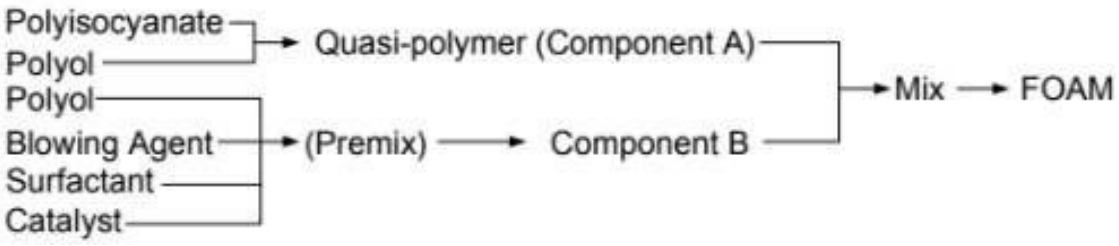

Figure I.3: Quasi pre polymer system

I.4 Types of polyurethane foam

Polyurethane foam is prepared by addition, condensation or cyclo-trimerization reactions. Polyurethane foam is divided into two main types: flexible foam and rigid foam. Each type is further categorized into multiple subtypes based on its applications. All types of polyurethane foams are prepared by appropriately selecting the polyol and isocyanate components. Table 1 illustrates the classification of polyurethane foam according to the type of polyol and its functionality.

Polyol	Rigid foam	Semi rigid foam	Flexible foam
OH No.	350-560	100-200	5.6-7.0
OH Equivalent No.	160-100	560-280	10,000-80
Functionality	3.0-8.0	3.0-3.5	2.0-3.1

Figure I.4: classification of polyurethane foam

I.4.1 FLEXIBLE POLYURETHANE FOAM

Flexible polyurethane foams are produced via either the slabstock or molding process, and their classification is based on both the synthesis method and the type of polyol employed. Slabstock-derived foams—commonly referred to as slabstock foams—are further categorized into several types:

polyether foam, high-resilience foam, viscoelastic foam, super-soft foam, energy-absorbing foam, and flexible polyester foam. In contrast, molded foams are divided into two distinct categories: hot-molded foam and cold-molded foam.

I.4.2 RIGID POLYURETHANE FOAM

”Rigid polyurethane foam is charverse range of density values. The synthesis of this foam typically occurs at ambient temperature, eliminating the need for external heating. Various specialized techniques are employed in its production, including spray foaming and one-component foaming. Furthermore, rigid foams are categorized into several forms, such as laminates, sandwich panels, high-density variants, and slab-stock foam. Additionally, both flexible and rigid foams can be synthesized on a laboratory scale through the cup foaming method.”[?]

I.5 Polyurethane Raw Materials

I.5.1 Polyols: Chemical Classification and Structure-Property Relationships

Polyols are macroglycols with terminal hydroxyl groups (-OH). In polyurethane chemistry, the functionality (f) and the hydroxyl number ($OH\#$) are the primary parameters defining the polymer network.

$$OH\# = \frac{56100 \times f}{M_n} \tag{I.1}$$

Polyether Polyols (The Hydrolytic Backbone)

Polyether polyols, such as Polypropylene Glycol (PPG), are synthesized via anionic ring-opening polymerization of alkylene oxides. They are characterized by ether linkages (C-O-C) which provide:

- **Low Glass Transition Temperature (T_g):** Facilitating flexibility at sub-zero temperatures.
- **Hydrolytic Stability:** Unlike esters, ether bonds do not react with water, making them ideal for humid environments.

Polyester Polyols (The High-Performance Backbone)

Synthesized through the condensation of diacids (e.g., Adipic acid) and diols. They offer superior:

- **Intermolecular Forces:** Higher hydrogen bonding potential leads to better tensile strength.
- **Abrasion Resistance:** Ideal for microcellular elastomers (shoe soles).

Table I.1: Comparative Analysis of Polyol Types in Materials Science

Property	**Polyether**	**Polyester**	**Polycaprolactone**
Hydrolytic Stability	Excellent	Poor	Moderate
Oxidative Stability	Poor	Excellent	Excellent
Tensile Strength	Moderate	High	Very High
Low Temp. Flexibility	Excellent	Moderate	Good
Typical Application	Flexible Foams	Coatings/Elastomers	High-end TPU

I.5.2 Isocyanates: Reactivity and Isomerism

Isocyanates are ester compounds of isocyanic acid, with the general structure R–N=C=O. They can be categorized based on the number of NCO groups, such as monoisocyanates (O=C=N–R–N=1) and polyisocyanates. Toluene diisocyanate (TDI) is the most widely produced and commonly used isocyanate in daily life.

TDI is mainly used in paints, adhesives, and flexible foams, with flexible foam accounting for 70% of its total consumption, followed by the coatings industry at 15%. Flexible polyurethane foam is found in furniture cushions, vehicle seat padding, and other soft cushioning layers. TDI is also used to produce rigid polyurethane foam, polyurethane coatings, and polyurethane elastomer intermediates.

MDI is classified into pure MDI, polymeric MDI, liquefied MDI, and modified MDI. TDI and MDI are interchangeable as raw materials for polyurethane production. Pure MDI is primarily used for slurry and polyurea spray, while polymeric MDI is used to produce polyurethane foam for insulation in refrigerators, water heaters, and similar appliances.

Polyphenylene polyisocyanate (PAPI), also known as crude MDI, is a mixture of MDI and polyisocyanates with more than two functional groups. It undergoes self-polymerization at high temperatures and can be used in polyurethane adhesives or added to rubber adhesives to enhance adhesion.

Other raw materials for polyurethane synthesis include HDI, XDI, and NDI. Xylylene diisocyanate (XDI) and naphthalene 1,5-diisocyanate (NDI) have limited applications and small production volumes in domestic industries. In contrast, 1,6-diisocyanate (HDI) offers excellent yellowing resistance and is increasingly replacing TDI in the coatings industry, particularly for high-grade automotive paints.[17]

I.5.3 Catalysts: The Gelling-Blowing Balance

The production of PU foam requires a precise synchronization between the gas evolution (blowing) and the molecular weight buildup (gelling).

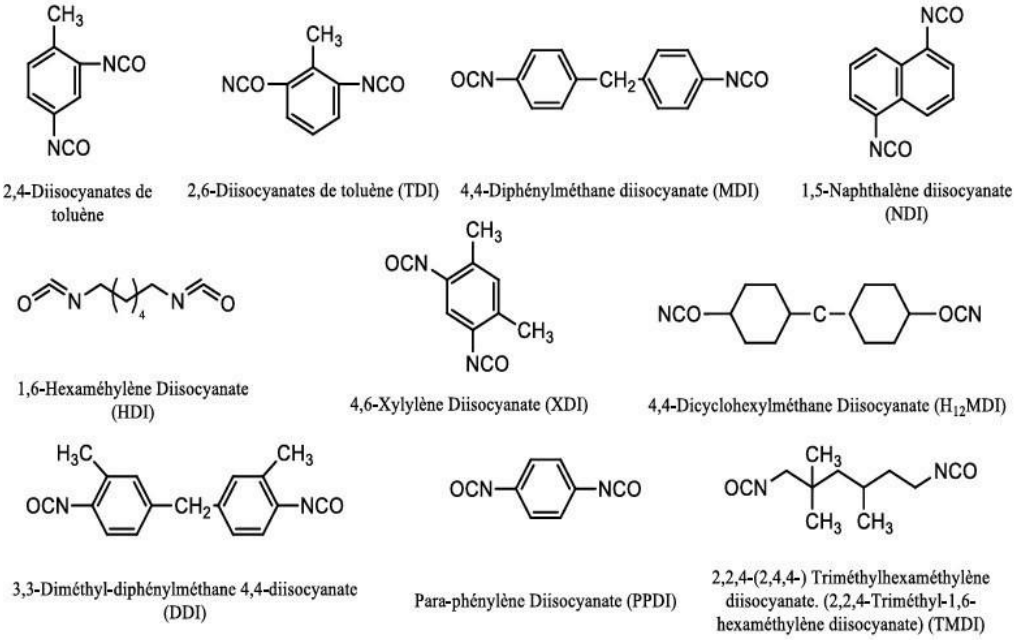

Figure I.5: Chemical Structures of Common Diisocyanates in Polyurethane Synthesis

Tertiary Amines (Blowing Catalysts)

Amines like Triethylenediamine (TEDA) or Bis(2-dimethylaminoethyl) ether catalyze the reaction between isocyanate and water. They operate by polarizing the water molecule, making the oxygen more nucleophilic.

Organometallic Catalysts (Gelling Catalysts)

Tin catalysts (e.g., Stannous Octoate) coordinate with the isocyanate group annomenon where the combined rate is faster than the sum of individual rates.

I.5.4 Surfactants: Silicone-Polyether Copolymers

Surfactants are essential to prevent ”Cell Collapse”. They perform three main functions:

- **Emulsification:** Combining the immiscible polyol and isocyanate phases into a quasi-homogeneous mixture.
- **Nucleation:** Lowering the surface tension (γ) to allow bubbles to form easily.
- **Surface Elasticity (Marangoni Effect):** Stabilizing the thin cell walls against drainage.

d the polyol hydroxyl group, bringing them into proximity to facilitate the urethane bond formation.
% Materials chemistry note:

I.6 castor oil

Chemical composition

The castor oil plant (Ricinus communis L.) is a widely cultivated crop with significant industrial applications, especially serving as a valuable and renewable resource for the chemical industry [1,2]. Castor oil, which is extracted from the plant's seeds through either cold or hot pressing, is both water-insoluble and water-resistant. The structure of the fatty acid within castor oil, particularly its functional group and position, enables a wide range of chemical reactions for industrial uses. This makes castor oil a key raw material for producing soaps, personal care products, lubricants, hydraulic and brake fluids, coatings, plastics, and polishes.

The oil's main components include ricinol, stearic, dihydroxy stearic, oleic, and linoleic acids, along with triacylglycerols. Castor oil appears as a yellow liquid with a characteristic taste and odor. It has a high density, which varies depending on its lipid content. The oil consists of a mixture of triglycerides, predominantly ricinoleate (around 90%), while oleate and linoleate are present in varying proportions.

Castor oil contains a distinctive and uncommon hydroxy fatty acid known as ricinolenic acid, which is structurally identified as cis-12-hydroxy-octadeca-9-ene acid (a hydroxyl fatty acid composed of 18 carbon atoms with one double bond)[18]

Figure I.6: Castor tree

Figure I.7: Castor oil

Origin of castor oil

Castor oil is derived from the seeds of a castor plant, also known as Ricinus communis, which forms part of the Euphorbiaceae family. The castor seeds usually contain up to 50% of the castor oil [1]. The castor plant is non-determinant, the seed grows at a different rate, hence resulting in harvesting

challenges, and the fact that the plant grows in rather difficult environments do not help because it also contributes to harvesting challenges. The other challenge is that the seed produces lipids with toxic ricin that can be considered to be an allergen, therefore making conventional harvesting a challenge and poisonous to harvesters. However, the composition of fatty acids in castor oil makes it worthwhile to harvest [19].

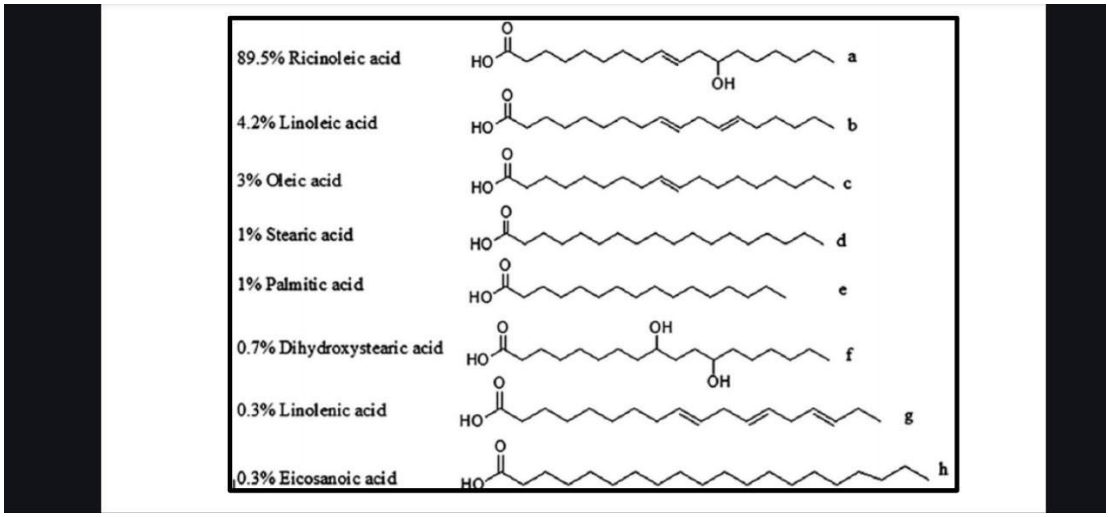

Figure I.8: Composition of castor oil fatty acid[1].

I.6.1 Physical and chemical properties

The physicochemical properties of castor oil, including specific gravity, refractive index, acid value, iodine value, saponification value, free fatty acid content, and pH, as reported in the literature, are summarized in Table .[20]

Physicochemical properties	Castor oil
specific gravity, 20_{25}	0.9610 g cm^{-3}
refractive index, n_D	1.4770
viscosity, η	630–880 mPa s
acidic value, mg KOH/50 g oil	0.4–4.0
iodine value, mg I_2/100 g oil	85.5
saponification value, mg KOH/100 g oil	180.3
free fatty acids, %	0.3–0.7
pH	6.00–7.00
melting point	−18.0 °C
boiling point	>300 °C

Figure I.9: Physical and chemical properties Castor oil

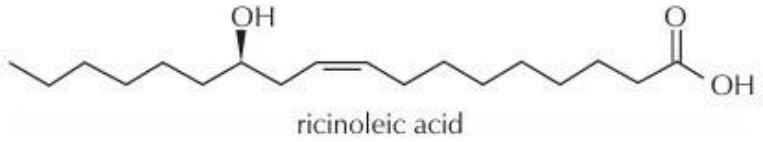

Figure I.10: ricinoleic acid

I.6.2 chemical modification of castor oil

The unique properties of castor oil can be manipulated from different chemical reactions by exploiting the different functional groups such as the ester linkage, hydroxyl group, and the vinyl group. These functional groups can be modified through processes such as transesterification, epoxidation, dehydration, pyrolysis, hydrogenation, ozonolysis, sulfation, and hydrolysis [21]. The chemical modifications of castor oil are clearly illustrated below (Figure I11). From the versatile list of processes to follow, the process should be energy efficient, green, and less labor intensive. This is because the aspects of health, safety, and environment need to be taken into account.

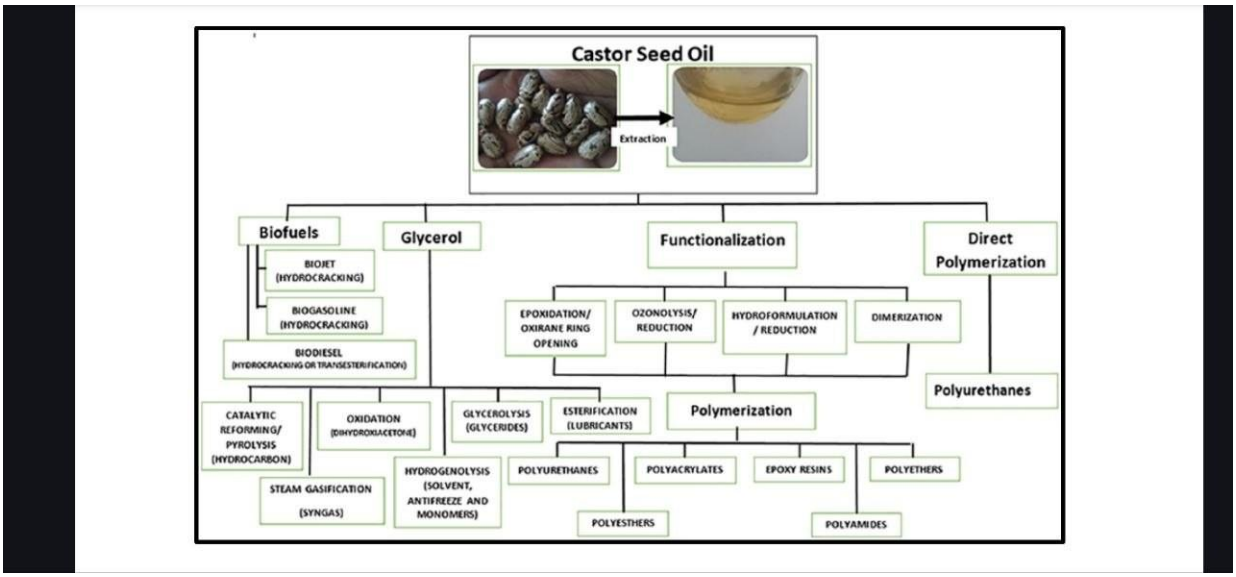

Figure I.11: Routes for the synthesis of various products from vegetable oils [2–4].

Chapter II

EXPERIMENTAL MATERIALS AND METHODS

II.1 Methodology experimental

II.1.1 Chemical Reagents Used

The chemical reagents used in this study are listed in Table

Table II.1: Physicochemical Properties and Suppliers of Used Chemical Reagents.

Product	**Chemical Formula**	**CAS N°**	**Density** ($g \cdot cm^{-3}$)	**M.W.** ($g \cdot mol^{-1}$)	**Supplier**
Toluene diisocyanate	$C_9H_6N_2O_2$	26471-62-5	1.22	174.16	Merck
Polypropylene Glycol PPG-10	$HO\text{-}[CH_2\text{-}CH(CH_3)\text{-}O]_n\text{-}H$	–	–	–	–
N,N-dimethyltrimethylenediamine	$C_5H_{14}N_2$	109-55-7	0.82	102.18	Merck
Tin Ethylhexanoate	$C_{16}H_{30}O_4Sn$	2417629-16-2	1.251	405.1	Fluka
trichloropropyl Phosphate	$C_3H_6Cl_3PO_4$	58888-75-8	–	243.41	Fluka
Siloxane-Polyether Copolymer	(Structure)	94469-32-6	–	–	Fluka
Water	H_2O	7732-18-5	1.00	18.015	–
Castor oil	**$C_{57}H_{104}O_9$**	**8001-79-4**	**0.957**	**933.46**	**–**

II.2 Polyurethane Foam preparation

The polyurethane foam was prepared according to the following experimental procedure:

1. A predetermined amount of polyols was introduced into a clean and dry glass beaker.
2. Trichloropropyl phosphate, distilled water, and siloxane–polyether copolymer were then gradually added to the polyol mixture.
3. Subsequently, the catalytic system composed of tin ethylhexanoate and N,N-dimethyltrimethylenediamine was incorporated into the formulation.

4. The resulting mixture was continuously stirred using a magnetic stirrer until a homogeneous system was obtained.

5. Toluene diisocyanate (TDI) was then added to the reactive medium under continuous stirring to ensure rapid homogenization.

6. Immediately after mixing, the reactive formulation was poured into an aluminum mold to allow foam expansion.

7. The foam was left to expand freely and cure at room temperature until complete solidification and stabilization were achieved.

The exact composition of the formulation is given below: [22]

Table II.2: Formulation and Volumetric Ratios of Chemical Reagents Used in PUF Synthesis.

Chemical Reagent	Volume Used (*mL*)
Polyols	20.0
Trichloropropyl phosphate	0.4
Water	1.0
Siloxane–polyether copolymer	0.4
Tin ethylhexanoate	0.1
N,N-dimethyltrimethylenediamine	0.1
Toluene diisocyanate (TDI)	12.0

II.3 Preparation of Polyurethane Foam Samples

Three formulations were developed using castor oil as the primary source of polyols, with the quantities of materials employed in each formulation presented below:

II.3.1 Formulation 01

- Polyols : 20mL Polypropylene Glycol PEG-10
- Trichloropropyl phosphate : 0.4 mL
- Water : 1 mL
- Siloxane-polyether copolymer : 0.4 mL
- Tin ethylhexanoate : 0.1 mL
- N, N-dimethyltrimethylenediamine: 0.1 mL
- TDI: 12 mL

II.3.2 Formulation 02

- Polyols : 10 mL Castor oil+ 10 mL Polypropylene Glycol PEG-10
- Trichloropropyl phosphate : 0.4 mL
- Water : 1 mL
- Siloxane-polyether copolymer : 0.4 mL
- Tin ethylhexanoate : 0.1 mL
- N, N-dimethyltrimethylenediamine: 0.1 mL
- TDI: 10 mL

II.3.3 Formulation 03

- Polyols : 20 mL castor oil
- Trichloropropyl phosphate : 0.4 mL
- Water : 1 mL
- Siloxane-polyether copolymer : 0.4 mL
- Tin ethylhexanoate : 0.1 mL
- N, N-dimethyltrimethylenediamine: 0.1 mL
- TDI: 10 mL

II.4 Physical and Chemical Characterization of PUFs

II.4.1 Density

The bulk density (ρ) of PU foams was performed according to ASTM D3574-03, Test A [2-3], the size of the samples was measured using a caliper and accurately weighted on a digital scale (Mettler Toledo, AB 265-S). The bulk density was calculated as the average mass/volume ratio of five regularly shaped samples.

II.4.2 Gravimetric Absorption

- **Materials:** Precision balance (0.1 mg), test liquid (water).
- **Procedure:**
- Weigh the dry foam (WdryWdry).
- Immerse in the liquid for 1 minute.
- Drain and reweigh (WwetWwet).
- Calculate the absorption

II.4.3 Average Functionality Calculation

The average functionality (f_{avg}) of the reaction mixture was calculated using the following equation:

$$f_{avg} = \frac{\sum n_i f_i}{\sum n_i} \tag{II.1}$$

where n_i is the number of moles of component i, and f_i is its functionality.

Equimolar Case

Assuming 1 mol of Ricinoleic acid ($f = 3$) and 1 mol of TDI ($f = 2$):

$$f_{avg} = \frac{(1 \times 3) + (1 \times 2)}{1 + 1} \tag{II.2}$$

$$f_{avg} = \frac{5}{2} = 2.5 \tag{II.3}$$

Therefore, the average functionality of the equimolar mixture is:

$$f_{avg} = 2.5 \tag{II.4}$$

Excess Ricinoleic Acid Case

Assuming 2 mol of Ricinoleic acid ($f = 3$) and 1 mol of TDI ($f = 2$):

$$f_{avg} = \frac{(2 \times 3) + (1 \times 2)}{2 + 1} \tag{II.5}$$

$$f_{avg} = \frac{8}{3} = 2.67 \tag{II.6}$$

Thus, the average functionality of the mixture is:

$$f_{avg} = 2.67 \quad \text{(II.7)}$$

The obtained values indicate that the average functionality is greater than 2, suggesting the formation of a branched and partially crosslinked polyurethane network. Increasing the proportion of Ricinoleic acid increases the average functionality, which may enhance the rigidity and thermal stability of the resulting polyurethane foam.

II.4.4 Spectroscopy Infrared analysis

The Fourier Transform Infrared (FTIR) spectra of the polyurethane foam samples were recorded using an Agilent Cary 630 FTIR spectrometer equipped with an ATR (Attenuated Total Reflectance) accessory. A small piece of each polyurethane foam sample was placed directly onto the ATR crystal and compressed using the pressure arm to ensure good contact with the crystal surface. Prior to each measurement, a background spectrum was collected under the same operating conditions. The spectra were acquired over the wavenumber range of 4000–650 cm^{-1} with a spectral resolution of 4 cm^{-1} and 32 scans per sample. After each analysis, the ATR crystal was cleaned with ethanol to avoid contamination between measurements. The obtained spectra were used to identify the characteristic functional groups of the synthesized polyurethane foams.

Figure II.1: Carry 630 FTIR Spectrometer by Agilent Technologies

II.5 Scanning electron microscopy (MEB/EDS) analysis

Scanning Electron Microscopy (SEM) is a widely employed technique for investigating the microstructure, cellular architecture, and surface morphology of polyurethane (PU) foams. Careful sample preparation is essential to minimize imaging artifacts and obtain high-quality micrographs. Since polyurethane foam is an electrically insulating material, a thin conductive coating must be applied prior to SEM observation to prevent surface charging and enhance image resolution. In this study,

the samples were coated with a thin layer (approximately 5–10 nm) of gold, gold–palladium alloy, or carbon using a sputter coater operated at a current of 20–30 mA for 60–120 s under an argon atmosphere. When performing Energy-Dispersive X-ray Spectroscopy (EDS) analysis, special attention should be paid to the coating thickness and composition to avoid interference with the detection and quantification of the sample's elemental constituents.

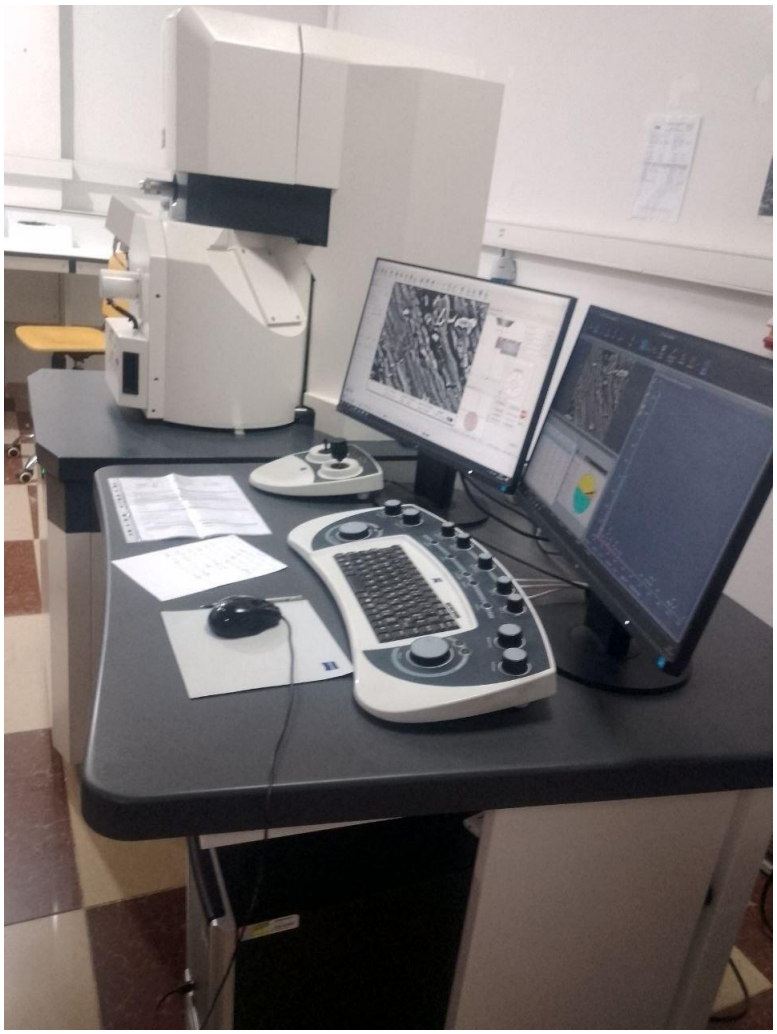

Figure II.2: Scanning electron microscopy (MEB/EDS)

II.5.1 SEM Imaging Parameters

Accelerating Voltage: 5–15 kV (lower voltages reduce beam penetration and enhance surface detail).

- Working Distance: 5–10 mm for optimal resolution.
- Detector: Secondary electron (SE) detector for surface topography; backscattered electron (BSE) detector for compositional contrast.

- Use a sharp blade or cryo-microtome to cut the PU foam into small, representative sections (typically 5–10 mm in width/height). Avoid compressing or tearing the foam during cutting to preserve cell structure.
- For rigid foams: Room-temperature cutting is sufficient.
- For flexible foams: Freeze the sample in liquid nitrogen for 5–10 minutes to harden it, enabling clean fractures without deformation.
- Remove debris or dust from the sample surface using compressed air or a soft brush.
- Avoid solvents unless necessary (e.g., ethanol for hydrophobic contaminants), as they may alter the foam's structure. The polyurethane foam samples were analyzed with a scanning electron microscope coupled with energy dispersive X-ray spectroscopy (SEM-EDX) .

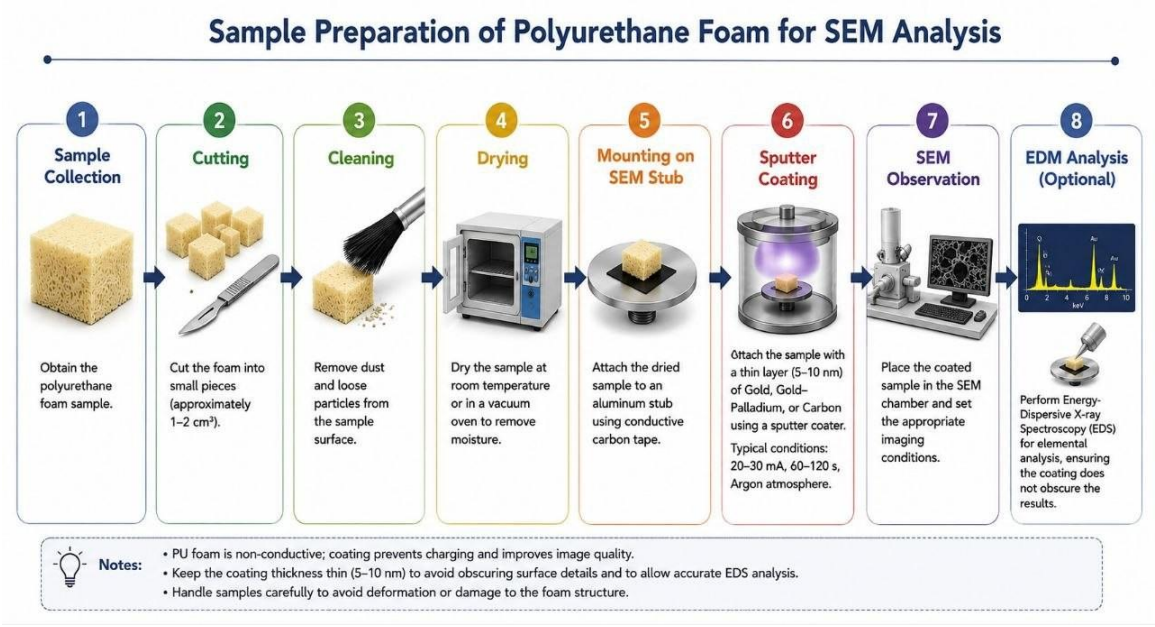

Figure II.3: Sample Preparation of Polyurethane Foam for SEM Analysis

II.5.2 Tensile test

Mechanical tensile tests were performed on a Mecmesin universal testing machine with a 10 kN capacity, with computer-controlled test software, and with a 10 kN force sensor and pneumatic grips. The ultimate tensile strength and percentage elongation at break were determined according to the ASTM D-3574-03 standard, Test E. The tests were conducted at a speed of 50 mm · min^{-1}. The tensile properties were measured in the rise direction of the foam and correspond to the average for at least three samples. The equipment used and the shape of the specimens cut from the foam blocks were selected in accordance with established standard specifications.

Figure II.4: Foam Compression Testing

Chapter III

RESULTS AND DISCUSSIN

III.1 Polyurethane Foam Synthesis

The synthesis reaction involving polypropylene glycol (PPG) and toluene diisocyanate (TDI) was conducted at room temperature under catalytic action of N,N-dimethyltrimethylenediamine and tin ethylhexanoate. The proposed reaction mechanism is shown below.[?]

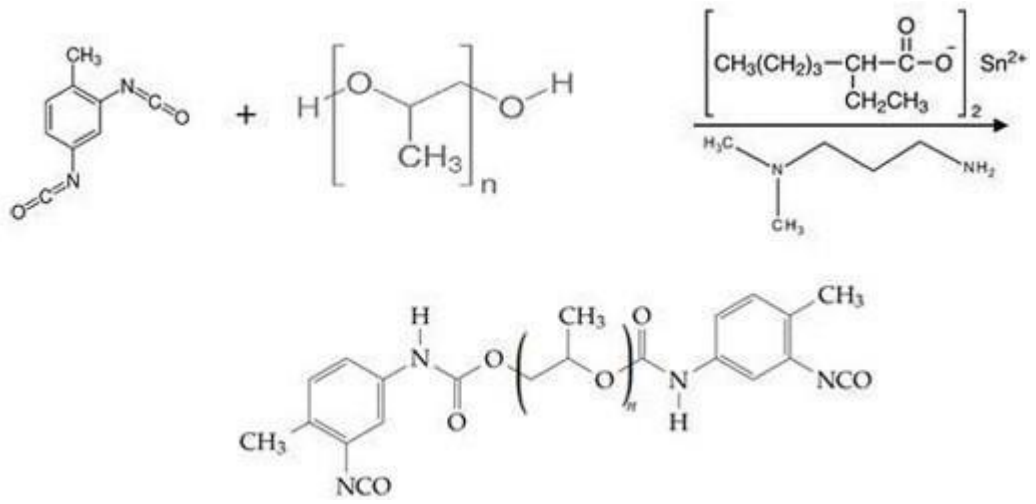

Figure III.1: Reaction schéma for the synthesis of polyurethane foam

III.1.1 Reactional mechanism

Isocyanates readily react with active hydrogen-containing compounds, and these reactions may be carried out with or without catalytic assistance. In contrast, isocyanate self-addition reactions are generally less favorable and occur less easily than reactions involving active hydrogen species.[?]

Reaction in the absence of a catalyst

The active compound itself serves as a catalyst during the reaction, as illustrated below.

As shown in Scheme , reactions occurring in the absence of a catalyst proceed through a nucleophilic addition mechanism. The nucleophilic center of the active hydrogen-containing compound attacks

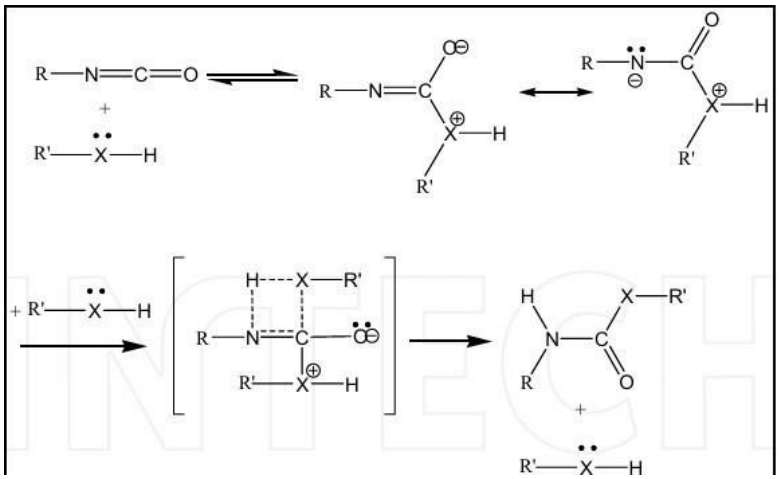

Figure III.2: Isocyanate reaction in the absence of a catalyst

the electrophilic carbon atom of the isocyanate group (–NCO), resulting in the formation of an intermediate that subsequently undergoes proton transfer. This process leads to the addition of hydrogen across the isocyanate group and the formation of the corresponding urethane linkage. The high reactivity of the –NCO group is mainly attributed to the strong electrophilic character of its carbon atom, which facilitates its interaction with nucleophilic species. The reactivity of isocyanates is strongly governed by the electronic and steric effects of the substituent groups present in their molecular structure. Electron-withdrawing substituents increase the electrophilic character of the carbon atom in the isocyanate group (–NCO), thereby enhancing its reactivity toward nucleophilic species. In contrast, electron-donating substituents reduce the electrophilicity of the isocyanate carbon and consequently decrease its reactivity. Furthermore, aromatic isocyanates generally exhibit greater reactivity than their aliphatic counterparts owing to the resonance and inductive effects associated with the aromatic ring. However, steric hindrance surrounding either the isocyanate group or the active hydrogen-containing reactant can significantly impede molecular interactions, resulting in a reduction in the reaction rate. In the absence of catalysts, the relative reactivity of active hydrogen-containing compounds toward isocyanates decreases in the following order: aliphatic amines, aromatic amines, primary alcohols, water, secondary alcohols, tertiary alcohols, phenols, carboxylic acids, ureas, amides, and urethanes. This reactivity sequence reflects the nucleophilicity and accessibility of the active hydrogen species involved in the addition reaction.[7]

III.2 Reaction in the presence of a catalyst

The isocyanate reactions classified under category (a) exhibit a high sensitivity to catalytic effects. The extent to which these reactions are accelerated depends on the nature of the catalyst employed. Consequently, catalyzed reactions are extensively utilized in industrial isocyanate-based processes. Among the most commonly used catalysts are tertiary amines and metal-containing compounds, particularly organotin derivatives, as previously discussed in this chapter. The catalytic pathways associated with

these reactions are illustrated in Figures 10 and 11, while their fundamental mechanisms remain comparable to those observed in the uncatalyzed reaction presented in Figure 9. The catalytic action of tertiary amines and metal salts on isocyanate reactions can be described as follows.

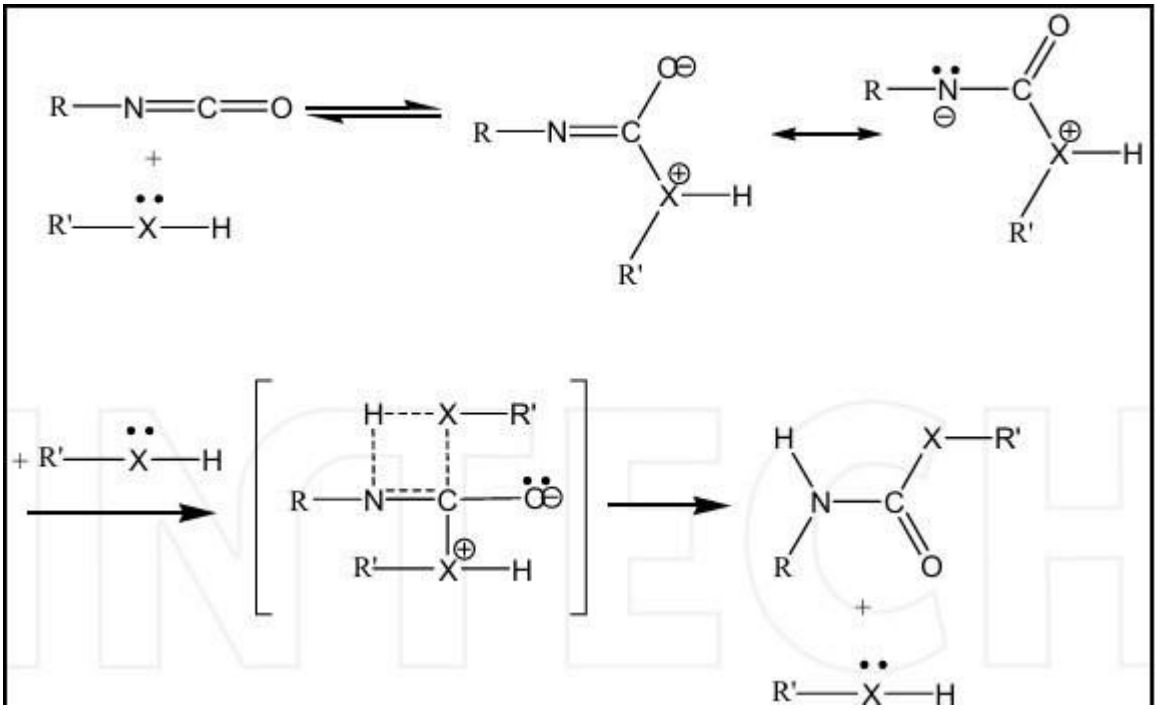

Figure III.3: Tertiary amine catalysed reaction

The catalytic efficiency of amine catalysts is generally correlated with their basicity, with higher basic strength leading to increased catalytic activity, provided that steric hindrance does not significantly interfere with the reaction. Amine catalysts are also effective in promoting the self-addition reactions of isocyanates. In contrast, metal salt catalysts usually exhibit a lower catalytic effect on these reactions, while tin-based compounds are considered particularly ineffective for facilitating self-addition processes.

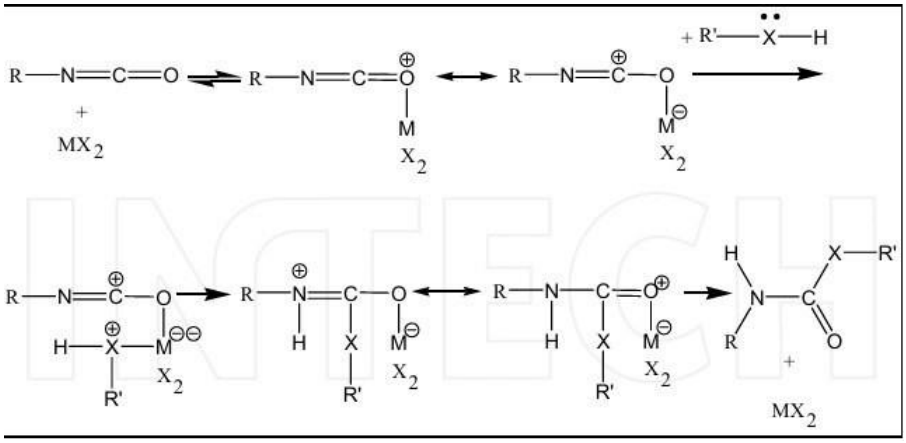

Figure III.4: Metal salts catalysed reaction

show the shapes of expanded polyurethane foams in aluminum molds, these foams are prepared from the synthetic polyol (PPG) and the biosource polyol (castor oil).

Figure III.5: Expanded polyurethane foams in aluminum molds

III.3 FTIR Analysis

III.3.1 FTIR Spectroscopy Analysis PU(1)

The FTIR spectrum of the synthesized polyurethane foam based on castor oil exhibits several characteristic absorption bands confirming the successful formation of the polyurethane network. A broad absorption band observed around 3300–3400 cm^{-1} is attributed to the stretching vibration of hydroxyl (O–H) and urethane N–H groups. The presence of this band indicates hydrogen bonding interactions within the polymer matrix.

The absorption bands located at approximately 2920 and 2850 cm^{-1} correspond to the asymmetric and symmetric stretching vibrations of aliphatic C–H bonds originating from the long fatty acid chains of castor oil. These peaks confirm the incorporation of the vegetable oil into the polymer structure.

The band observed in the region of 1700–1730 cm^{-1} is assigned to the carbonyl stretching vibration (C=O) of the urethane groups, representing one of the most important indicators of polyurethane

formation. Furthermore, the absorption bands between 1600 and 1500 cm^{-1} are associated with N–H bending vibrations and C–N stretching of the urethane linkage.

The intense absorption peak observed around 1100–1000 cm^{-1} is attributed to C–O–C and C–O stretching vibrations, which are characteristic of ester and urethane functionalities derived from castor oil and the polyurethane network. Additional bands below 900 cm^{-1} correspond to out-of-plane bending vibrations of C–H bonds and other skeletal vibrations of the polymer chain.

Overall, the FTIR analysis confirms the successful synthesis of polyurethane foam from castor oil through the formation of urethane linkages (–NH–COO–). The presence of characteristic hydroxyl, carbonyl, amine, and ether groups demonstrates the effective reaction between the hydroxyl groups of castor oil and the isocyanate groups, leading to the development of a crosslinked polyurethane structure.

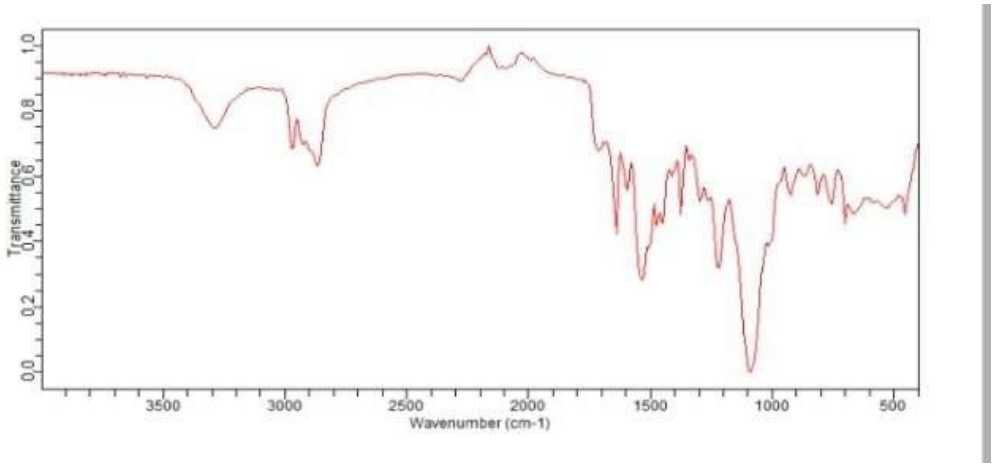

Figure III.6: FTIR Spectroscopy PU(1)

III.3.2 FTIR Spectroscopy Analysis PU(2)

The FTIR spectrum of Sample PU2 confirms the successful synthesis of polyurethane foam from castor oil through the reaction between hydroxyl groups of the polyol and isocyanate groups. A broad absorption band centered around 3300–3400 cm^{-1} is observed and assigned to the stretching vibrations of hydroxyl (O–H) and urethane (N–H) groups. This band indicates the presence of hydrogen bonding interactions within the polymer network.

The absorption bands appearing at approximately 2920 and 2850 cm^{-1} correspond to the asymmetric and symmetric stretching vibrations of aliphatic C–H bonds, originating from the fatty acid chains of castor oil. These peaks confirm the incorporation of the renewable vegetable oil into the polyurethane structure.

A characteristic absorption band observed near 1700–1730 cm^{-1} is attributed to the carbonyl (C=O) stretching vibration of urethane groups. The appearance of this peak provides strong evidence for the formation of urethane linkages during polymerization. In addition, absorption bands located around

1600–1500 cm^{-1} are associated with N–H bending and C–N stretching vibrations, which are typical of polyurethane materials.

The most intense absorption bands are observed in the 1250–1000 cm^{-1} region and correspond to C–O–C and C–O stretching vibrations of ester and urethane functionalities. The high intensity of these peaks indicates the development of a highly crosslinked polyurethane network. Additional bands below 900 cm^{-1} are related to skeletal vibrations of the polymer backbone and out-of-plane bending of C–H bonds.

Furthermore, the absence or significant reduction of the isocyanate absorption band around 2270 cm^{-1} suggests that most of the NCO groups were consumed during the polymerization reaction, confirming the successful formation of polyurethane foam.

Overall, the FTIR results demonstrate the formation of a polyurethane structure containing urethane, ester, hydroxyl, and aliphatic functional groups, confirming the effective utilization of castor oil as a renewable polyol source in polyurethane foam production.

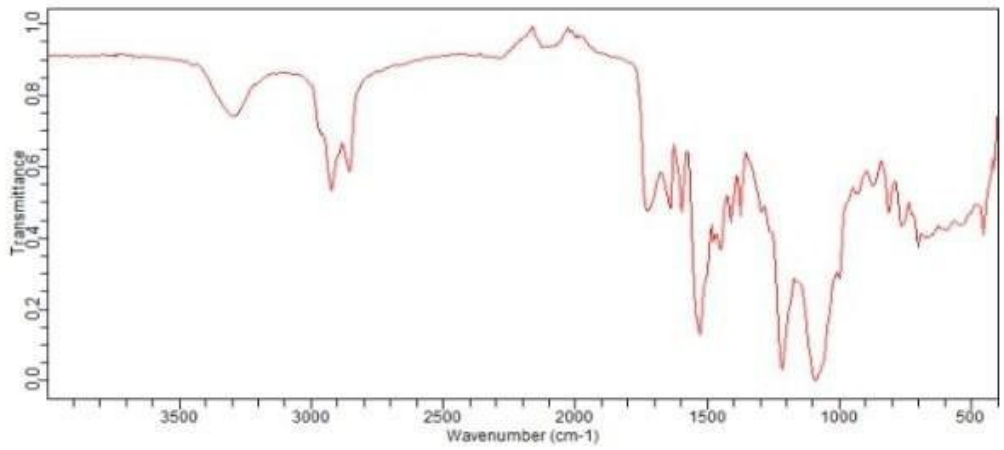

Figure III.7: FTIR Spectroscopy PU(2)

III.3.3 FTIR Spectroscopy Analysis PU(3)

The FTIR spectrum of Sample PU 3 exhibits the characteristic absorption bands of castor oil-based polyurethane foam, confirming the successful formation of urethane linkages within the polymer matrix. A broad absorption band centered around 3300–3400 cm^{-1} is attributed to the stretching vibrations of N–H and residual O–H groups involved in hydrogen bonding interactions. The presence of this band is a typical feature of polyurethane materials.

The absorption peaks located near 2920 and 2850 cm^{-1} correspond to the asymmetric and symmetric stretching vibrations of aliphatic C–H bonds associated with the long hydrocarbon chains of castor oil. These peaks indicate the incorporation of the bio-based polyol into the polymer structure.

A distinct absorption band observed around 1700–1725 cm^{-1} is assigned to the carbonyl (C=O) stretching vibration of the urethane group. This peak confirms the reaction between hydroxyl groups

and isocyanate groups, leading to the formation of the polyurethane network. The bands appearing between 1600 and 1500 cm^{-1} are related to N–H bending and C–N stretching vibrations, which further support the presence of urethane linkages.

Strong absorption bands observed in the 1250–1000 cm^{-1} region are attributed to C–O–C and C–O stretching vibrations of ester and urethane groups. The increased intensity of these peaks suggests a higher degree of crosslinking and improved polymer network formation. Additional bands below 900 cm^{-1} are associated with skeletal vibrations of the polymer backbone and out-of-plane C–H bending vibrations.

The absence of a significant absorption band around 2270 cm^{-1}, corresponding to the isocyanate group (–NCO), indicates that the isocyanate was largely consumed during the polymerization process. Therefore, the FTIR spectrum confirms the successful synthesis of polyurethane foam from castor oil and demonstrates the formation of a stable crosslinked polymeric structure.

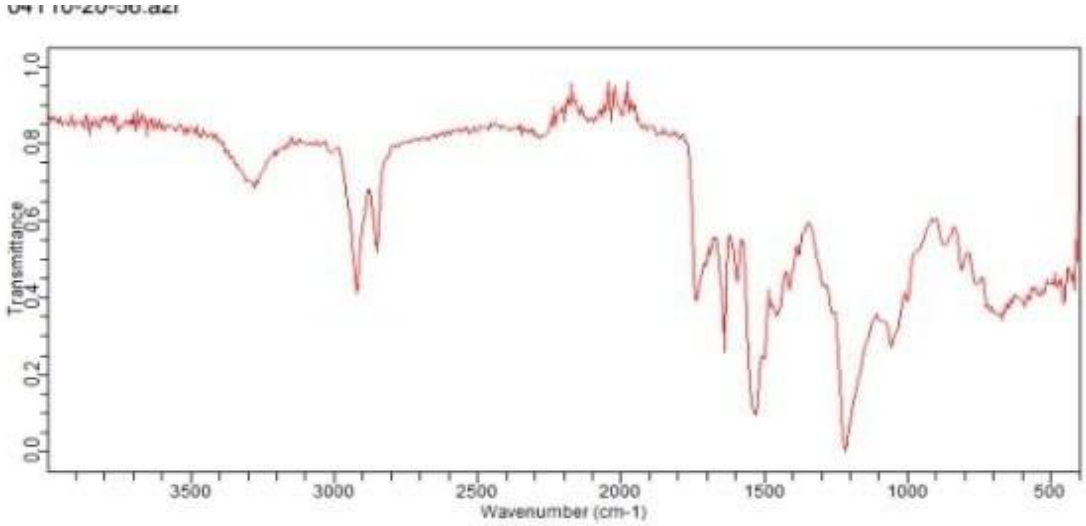

Figure III.8: FTIR Spectroscopy PU(3)

III.4 Physicochemical characterization of PUF

III.4.1 Gravimetric Absorption Test

$$\text{Absorption (\%)} = \frac{W_{wet} - W_{dry}}{W_{dry}} \times 100$$

According to the above equation, the absorption percentage was calculated.

Analysis of Water Absorption Results

The water absorption results presented in Table X reveal significant differences among the prepared polyurethane foam samples. These variations indicate differences in pore structure, cell morphology,

and the degree of cell openness within the foams. Sample PU1 exhibited the highest water absorption value (913%), indicating a highly porous structure with a large number of interconnected open cells. Such a structure facilitates water penetration and retention within the foam matrix, resulting in a remarkably high absorption capacity. In contrast, PU2 showed the lowest water absorption (244%), suggesting a denser and less porous structure. The reduced water uptake may be attributed to a lower proportion of open cells and limited pathways for water diffusion into the material. Sample PU3 displayed an intermediate absorption value (569%), reflecting a moderate level of porosity and water-retention capability compared with PU1 and PU2. The D30 sample achieved a water absorption of 649%, which is higher than that of PU3 but lower than that of PU1. This result suggests that the incorporation of D30 modified the internal foam structure, increasing the accessibility of water through enhanced pore connectivity or a greater number of open cells. Overall, the water absorption capacity followed the order: PU1 (913%) > D30 (649%) > PU3 (569%) > PU2 (244%) These findings demonstrate that water absorption is strongly influenced by the foam morphology. Samples with higher porosity and a greater proportion of open cells tend to absorb more water, whereas denser structures exhibit lower absorption capacities. This behavior is characteristic of polyurethane foams and plays an important role in determining their suitability for applications involving moisture absorption, filtration, or insulation.

	Wdry (g)	*Wwet (g)*	*A(%)*
PU1	*1.8678*	*18.9228*	*913*
PU2	*1.9526*	*6.7207*	*244*
PU3	*2.2374*	*14.9741*	*569*
D30	*1.9175*	*14.3665*	*649*

Figure III.9: Evaluation of Water Absorption in PU and D30 Foam Materials

III.4.2 Density

According to ASTM D3574-03, the bulk density was determined by calculating the average mass-to-volume ratio of three regularly shaped specimens, as presented in Table X.

analysis

The results presented in Table X show that the density values of the prepared polyurethane foam samples ranged from 0.0197 to 0.0378 g/cm³, with an average density of 0.0271 g/cm³. Sample PU2 exhibited the highest density (0.0378 g/cm³), indicating a more compact cellular structure with fewer internal voids. In contrast, sample PU3 showed the lowest density (0.0197 g/cm³), suggesting a higher degree of foam expansion and a larger amount of entrapped air. Sample PU1 displayed an intermediate

Sample N°	Volume (cm-1)	Mass (g)	Density (g. cm-1)
PU1	50.4	1.2111	0.0240
PU2	37.62	1.4227	0.0378
PU3	45	0.8909	0.0197
Average	_	_	0.0271

Figure III.10: Bulk Density of Polyurethane Foam Samples.

density value (0.0240 g/cm³). The low average density confirms the lightweight nature of the synthesized polyurethane foam, which is a desirable characteristic for thermal insulation and cushioning applications. Variations in density are mainly attributed to differences in cell morphology, expansion behavior, and foam formation conditions.

comparison

Based on the data presented in the table, the average density of the laboratory-prepared samples (PU1, PU2, and PU3) is 0.0271 g/cm³, whereas the density of the commercial sample D30 is 0.0389 g/cm³. Comparison:

- The commercial sample D30 exhibits a density approximately 43.5% higher than the average density of the laboratory-prepared samples.
- Among the laboratory samples, PU2 (0.0378 g/cm³) shows the closest density value to that of the commercial sample, although it remains slightly lower.
- PU1 and PU3 display significantly lower densities compared to D30. Factors Affecting Density:

  - Porosity: An increase in the volume of air-filled voids within the foam structure leads to a reduction in density. The laboratory-prepared samples appear to be more porous than the commercial sample.
  - Preparation Method: Processing parameters such as mixing speed, applied pressure during fabrication, and reaction temperature can significantly influence the final density.
  - Raw Material Composition: The type of polymer matrix and the presence of additives, fillers, or plasticizers may affect the foam density.
  - Curing Conditions: Factors including curing time, humidity, and entrapped air bubbles can alter the density of the final material.
  - Measurement Accuracy: The determination of density depends on accurate measurements of both mass and volume. It should be noted that the volume unit reported in the table as cm^{-1} appears to be incorrect; the correct unit is cm^3. To obtain a density closer to that of the commercial D30 sample, it is recommended to prepare samples under conditions similar to those used

for PU2 while minimizing porosity and optimizing processing parameters to promote a more compact foam structure.

III.5 SEM-EDX analysis

III.5.1 SEM analysis

Sample 1

The SEM micrographs of Sample 1 reveal a well-developed cellular structure characteristic of polyurethane foam. The cells exhibit predominantly oval and closed-cell morphology with relatively smooth cell walls and limited structural defects. At higher magnifications, the polymer matrix appears homogeneous, indicating good compatibility between the reactants and successful foam formation. The absence of significant cracks or voids suggests adequate structural integrity, which can contribute positively to the mechanical performance and thermal insulation properties of the foam.

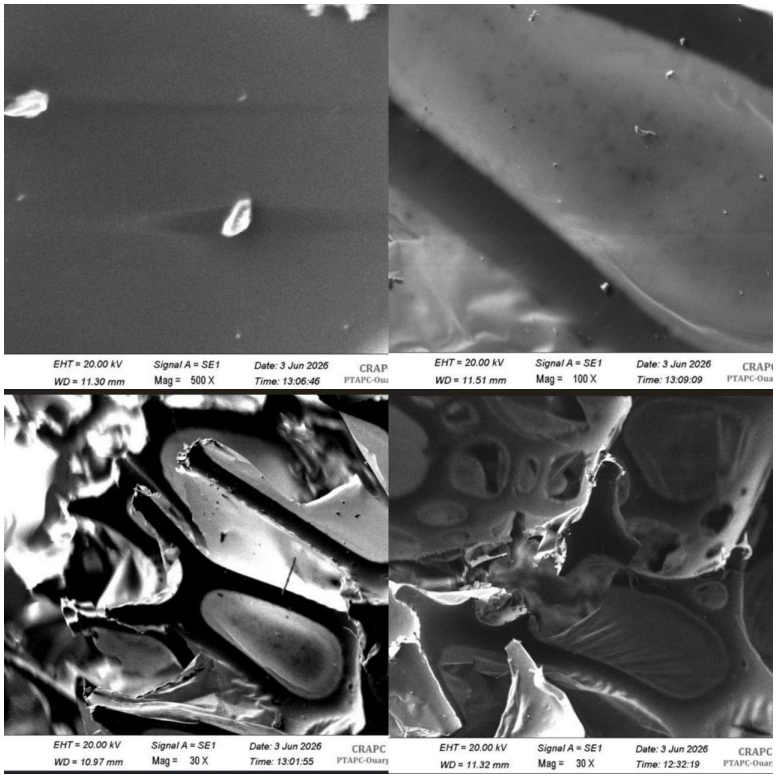

Figure III.11: SEM Micrographs of Sample 1 at Different Magnifications (30×, 100× and 500×).

Sample 2

SEM micrograph of the polyurethane foam reveals a highly porous cellular structure characterized by irregularly shaped and distributed cells. Both open and partially closed cells can be observed, indicating successful foam formation during the polymerization process. Some cell walls appear ruptured

or collapsed, suggesting local structural deformation caused by gas expansion, processing conditions, or sample preparation. The relatively large interconnected pores indicate high porosity, which may enhance water absorption and insulation properties. However, the non-uniform cell size distribution and wall defects may negatively affect the mechanical performance of the foam, particularly its compressive strength and structural stability.

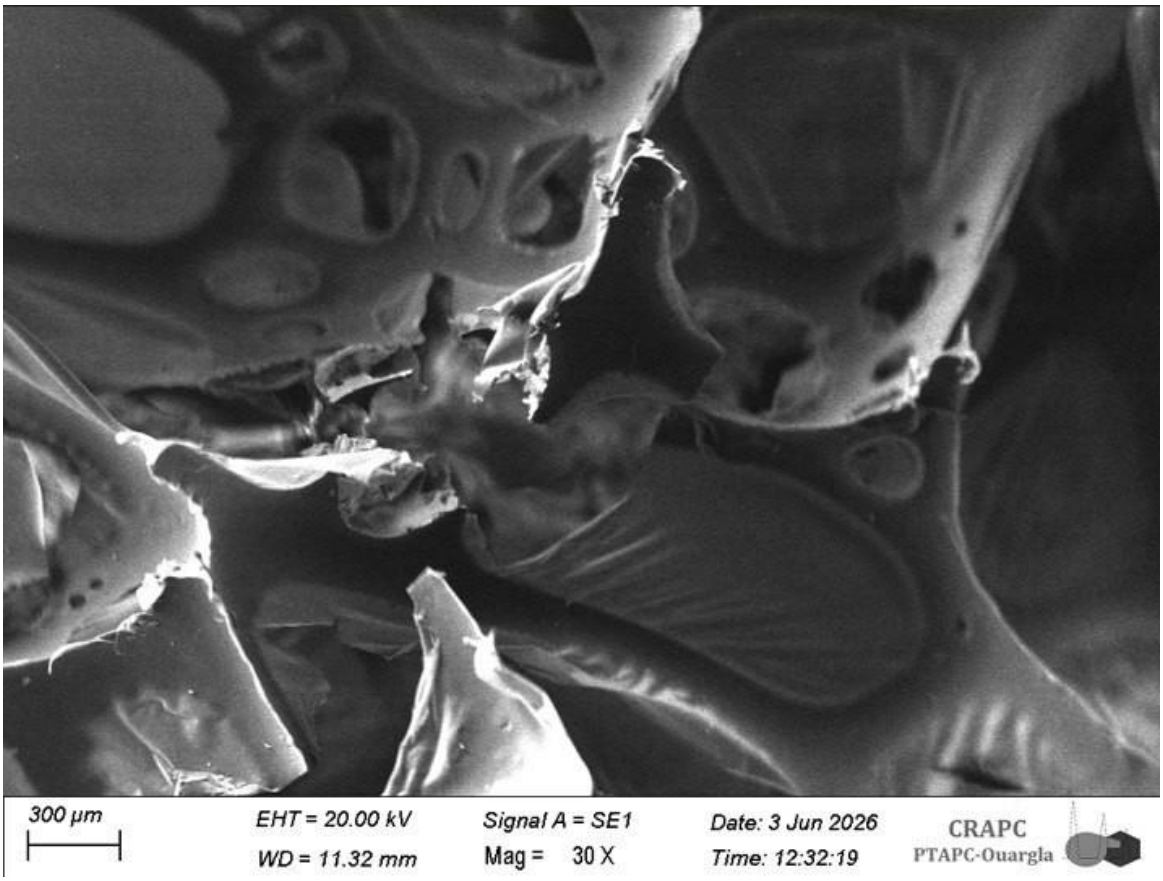

Figure III.12: SEM micrograph of sample2 showing the cellular morphology of polyurethane foam at 30× magnification.

Sample 3

The SEM micrographs of Sample 3 at different magnifications (30×, 100×, and 1000×) reveal a heterogeneous cellular structure with irregularly shaped pores and cell walls. At low magnification, the foam exhibits interconnected cellular domains with some collapsed regions. Increasing magnification shows relatively thick and compact cell walls, indicating the formation of a dense polymeric network. At 1000× magnification, the cell wall surface appears relatively smooth with only a few microvoids and surface defects, suggesting good polymerization homogeneity. The compact morphology and reduced pore openness are expected to enhance the mechanical properties and dimensional stability of the foam while reducing water uptake.

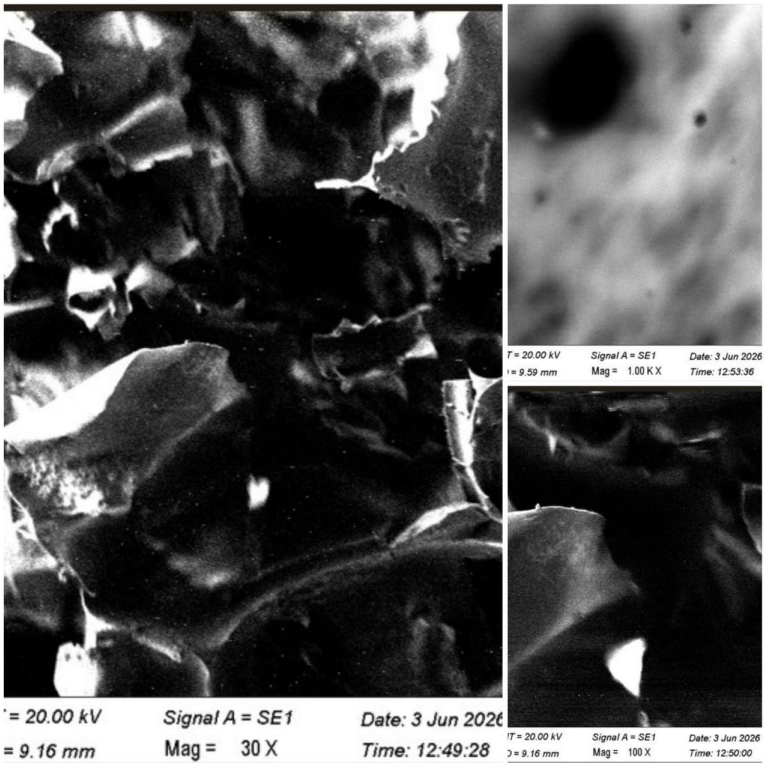

Figure III.13: SEM micrographs of Sample 3 at different magnifications (30×, 100× and 1000×), showing the cellular morphology of the synthesized polyurethane foam.

III.5.2 EDX analysis

sample 1

Elemental Composition Analysis (EDX Spectrum and Table) The energy-dispersive X-ray spectroscopy confirms the chemical signature of the polymer matrix: Matrix Elements (Primary Components):
Carbon (C): Accounting for 69.89 wt% (76.58 at%).
Oxygen (O): Accounting for 28.23 wt% (23.23 at%). Interpretation: The absolute predominance of C and O represents the typical organic backbone of polyurethane ([-O-R-O-CO-NH-R'-NH-CO-]n).
Secondary Elements andz Artifacts:
Gold (Au): Detected at 1.67 wt%. Interpretation: This is an artifact from the sample preparation process. Polyurethane is a non-conductive polymer, requiring a thin gold sputter coating prior to SEM imaging to prevent surface charging.
Silicon (Si): Detected at a trace level of 0.15 wt%. Interpretation: Commonly originates from silicone-based surfactants used as cell stabilizers during the foam formulation.
Niobium (Nb): Present in a negligible trace amount (0.06 wt%), likely a background signal from the SEM chamber hardware or a trace catalyst impurity.

"SEM/EDX analysis confirms the characteristic cellular matrix of polyurethane foam, showing signs of brittle cell wall cleavage. The EDX spectrum verifies the polymeric nature of the sample via dominant Carbon and Oxygen peaks (98 wt% combined), with minor Silicon traces from production

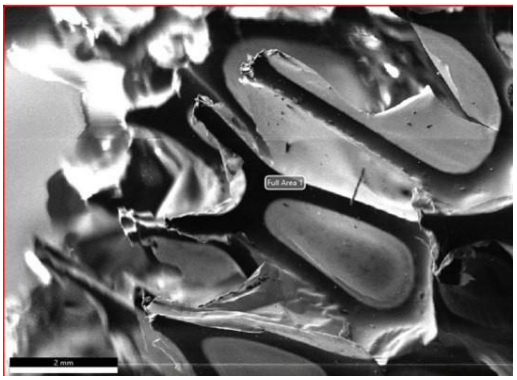

Figure III.14: SEM micrograph showing the cellular microstructure of Sample 1 with the designated analysis zone.

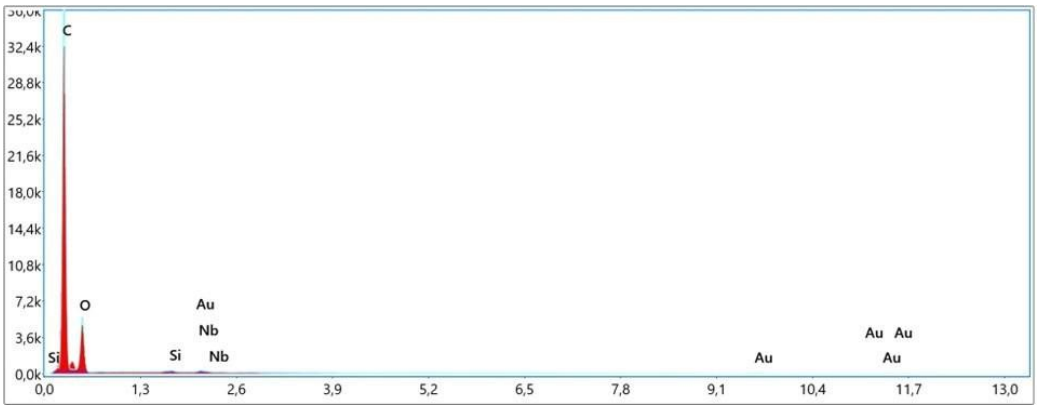

Figure III.15: EDX spectrum showing the elemental energy peaks for Sample 1.

Elément	% de masse	% atomique	Kratio	Z	A	F
C K	69.89	76.58	0,4947	1.0186	0.6949	1.0000
O K	28.23	23.23	0,0413	0.9734	0.1501	1.0000
SiK	0.15	0.07	0,0012	0.8830	0.8699	1.0042
NbL	0.06	0.01	0,0005	0.6825	1.1859	0.9996
AuL	1.67	0.11	0,0090	0.4942	1.0484	1.0415

Figure III.16: EDX spectrum showing the elemental energy peaks for Sample 1.

stabilizers and a distinct Gold peak introduced via the conductive sputter-coating required for high-resolution electron imaging."

sample 2

The EDX data presents the core polymeric matrix along with a few distinct elemental shifts: Matrix Elements (Primary Components):
Carbon (C): 66.18 wt% (73.86 at%).
Oxygen (O): 30.78 wt% (25.79 at%). Note: Compared to Sample 1, Sample 2 shows a slight decrease in Carbon and a corresponding increase in Oxygen content, though they still dictate the bulk organic

polyurethane structure (97 wt%). Secondary Elements Coating Artifacts:
Gold (Au): Detected at 2.21 wt% (higher than Sample 1), confirming a slightly thicker conductive sputter-coating layer on this specific sample surface. Palladium (Pd): Detected at 0.36 wt%. Interpretation: Pd is commonly alloyed with Gold target sources (Au/Pd targets) in sputter coaters to achieve a finer grain size for high-resolution SEM imaging. Calcium (Ca) Copper (Cu): Detected at trace levels (0.22 wt% and 0.12 wt% respectively). These likely point to mineral fillers, catalyst residues, or minor impurities introduced during foam synthesis or sample handling. Silicon (Si): Stable at trace levels (0.13 wt%), originating from silicone surfactant stabilizers.
Niobium (Nb): Dropped to 0.00 wt% (undetectable).

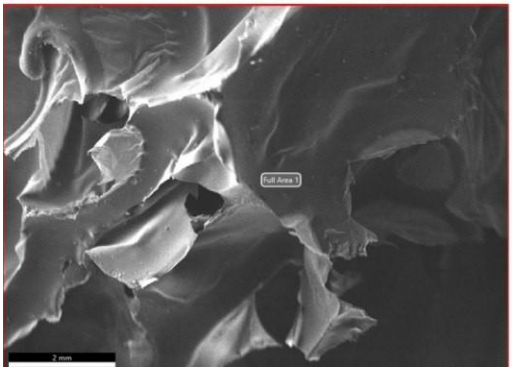

Figure III.17: SEM micrograph showing the deformed and ruptured cellular microstructure of Sample 2 within the designated analysis zone .

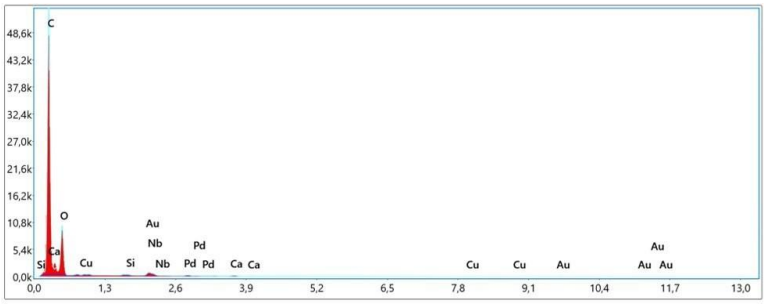

Figure III.18: EDX spectrum highlighting the elemental energy peaks and the presence of coating alloys (Au/Pd) for Sample

Elément	% de masse	% atomique	Kratio	Z	A	F
C K	66.18	73.86	0,4561	1.0233	0.6734	1.0000
O K	30.78	25.79	0,0477	0.9781	0.1586	1.0000
SiK	0.13	0.06	0,0010	0.8877	0.8605	1.0040
NbL	0.00	0.00	0,0000	0.6862	1.1712	0.9998
PdL	0.36	0.05	0,0028	0.6617	1.1731	1.0009
CaK	0.22	0.07	0,0019	0.8374	1.0187	1.0386
CuK	0.12	0.03	0,0013	0.7139	1.0160	1.4514
AuL	2.21	0.15	0,0119	0.4973	1.0496	1.0338

Figure III.19: Quantitative elemental composition (wt% and at%) of Sample 2 obtained from

EDX ”SEM/EDX characterization of Sample 2 reveals a ruptured cellular matrix with notable wall

folding

and fragmentation. EDX analysis confirms the polyurethane composition via dominant Carbon and Oxygen signals (97 wt% combined). The elemental spectrum uniquely captures a minor Palladium (Pd) peak alongside Gold (Au), indexing the use of a fine-grained Au/Pd conductive coating, with negligible traces of Calcium, Silicon, and Copper inherently tied to processing additives or residual impurities."

sample 3

The elemental profile reveals the raw organic matrix configuration along with distinct processing footprints: Matrix Elements (Primary Components):
Carbon (C): Highest concentration at 72.88 wt% (78.89 at%).
Oxygen (O): Accounting for 25.07 wt% (20.37 at%). Interpretation: Together, C and O compromise nearly 98 wt% of the scanned volume. The net increase in Carbon is due to the pristine exposed state of the polymer backbone. Absence of Coating Elements:
Gold (Au) and Palladium (Pd) peaks are completely absent from both the spectrum and the quantitative table, verifying the lack of a conductive sputter-coated layer which induced the SEM charging artifacts. Secondary Elements Impurities:
Niobium (Nb): Noticeably higher at 0.69 wt%.
Sodium (Na) Chlorine (Cl): Detected at 0.66 wt% and 0.28 wt% respectively. The correlated presence of Na and Cl suggests minor NaCl (salt) contamination during sample handling or preparation.
Silicon (Si) Calcium (Ca): Persist at minor trace background levels (0.22 wt% and 0.21 wt%), originating from foam processing additives.

Figure III.20: SEM micrograph of the surface morphology for Sample 3.

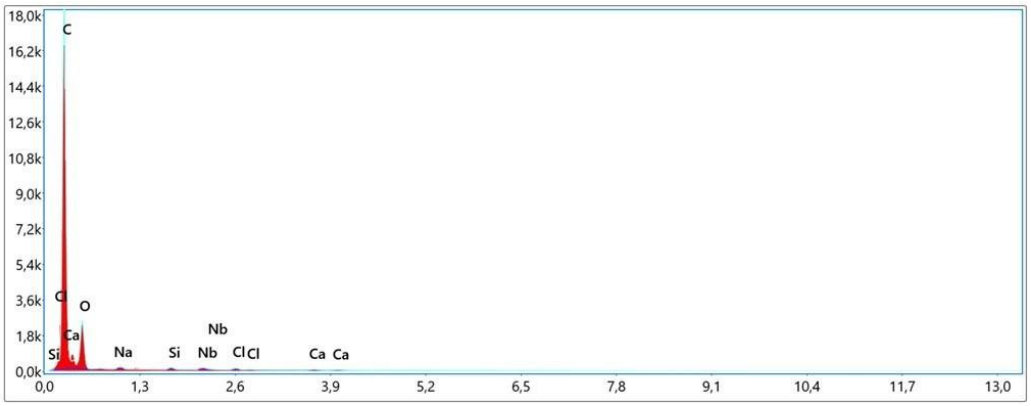

Figure III.21: EDX spectrum showing elemental peaks for Sample 3.

Elément	% de masse	% atomique	Kratio	Z	A	F
C K	72.88	78.89	0,4882	1.0147	0.6603	1.0000
O K	25.07	20.37	0,0340	0.9694	0.1398	1.0000
NaK	0.66	0.37	0,0025	0.8790	0.4370	1.0012
SiK	0.22	0.10	0,0017	0.8788	0.8741	1.0064
NbL	0.69	0.10	0,0056	0.6792	1.2013	1.0002
ClK	0.28	0.10	0,0024	0.8181	1.0070	1.0171
CaK	0.21	0.07	0,0018	0.8285	1.0333	1.0442

Figure III.22: Quantitative EDX elemental analysis table for Sample 3.

III.6 Tansil test

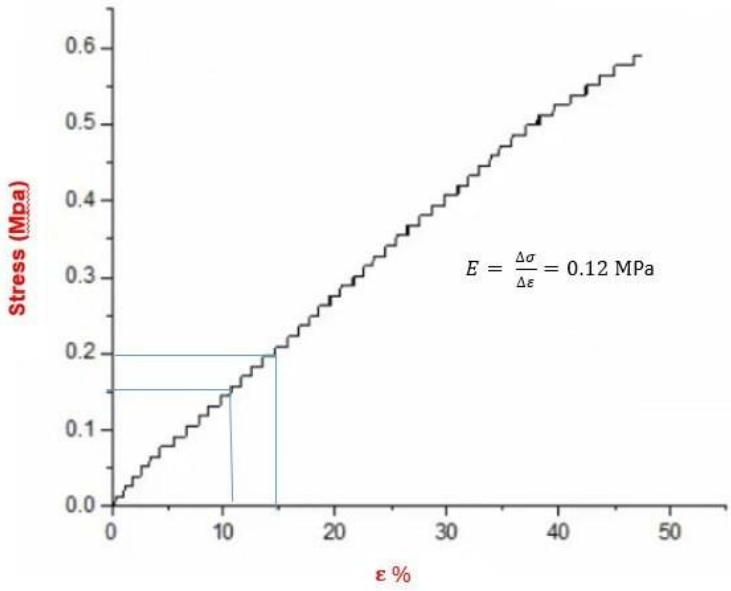

Figure III.23: Stress–strain curve of the prepared polyurethane foam showing the determination of Young's modulus (E = 0.2 MPa).

The polyurethane foam's stress-strain curve shows linear behavior until sudden failure, from which the elastic modulus (E) and ultimate tensile strength were determined.

The stress–strain curve of the polyurethane foam sample exhibits a mechanical behavior characterized by a gradual increase in stress with increasing strain. The initial portion of the curve shows a nearly linear relationship corresponding to the elastic region of the material, where the Young's modulus was determined to be approximately 0.12 MPa, reflecting the elastic nature and low-density cellular structure of the foam. As the applied load increased, the stress continued to rise without the appearance of a distinct yield point, which is a typical behavior of polymeric foams. The maximum tensile stress reached approximately 0.59 MPa at a strain close to 50%, indicating the ability of the sample to withstand significant deformation prior to failure. This behavior can be attributed to the flexibility of the polyurethane network and the progressive stretching and opening of the internal cellular structure during tensile loading.

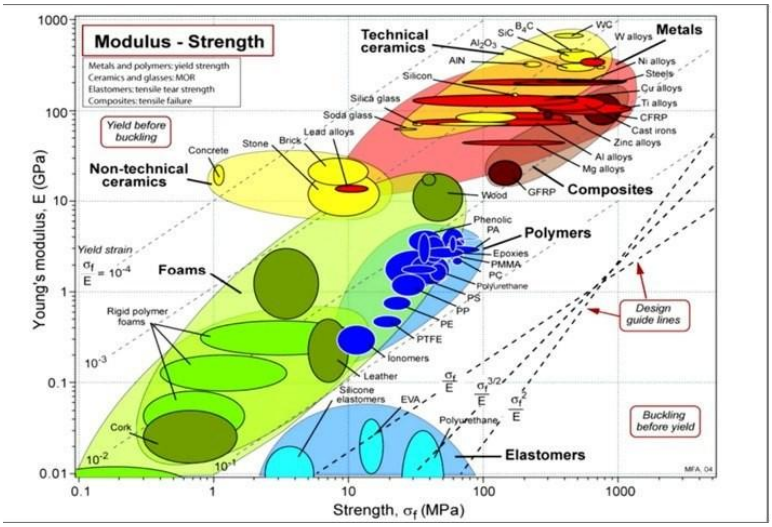

Figure III.24: Ashby chart showing the relationship between Young's modulus and strength for different classes of engineering materials.

presents an Ashby modulus–strength chart, which compares the mechanical properties of different classes of engineering materials. The chart correlates Young's modulus with tensile strength and illustrates the relative position of foams, polymers, metals, ceramics, and composites. Polyurethane foams are located in the low-modulus and low-strength region due to their highly porous cellular structure. This behavior is consistent with the experimental results obtained in the present work, where the synthesized polyurethane foam exhibited a Young's modulus of approximately 0.12 MPa and a tensile strength of about 0.59 MPa. The low stiffness and strength are mainly attributed to the low density and high porosity of the foam, which promote lightweight characteristics and energy absorption capabilities.

CONCLUSION

The study successfully demonstrates that castor oil serves as a viable, bio-sourced alternative to synthetic polyol (PPG) in producing polyurethane foams (PUFs). By altering the polyol formulation, the ratio of open-to-closed cells can be precisely controlled, allowing manufacturers to tailor the foam's physical, morphological, and mechanical properties for specific industrial applications.

Key Formulation Outcomes and Applications The Hybrid Blend (PU2 – Castor Oil + PPG): * Characteristics: Exhibited the highest density and lowest water absorption due to a compact, less porous structure. Best Suited For: Rigid insulation applications requiring structural density and water resistance. The Pure Synthetic Foam (PU1 – 100% PPG): * Characteristics: Recorded the highest water absorption (913%), indicating a highly porous network of interconnected open cells. Best Suited For: Absorption and filtration systems where liquid penetration is required. The Pure Bio-Based Foam (PU3 – 100% Castor Oil): * Characteristics: Offered an intermediate solution with the lowest apparent density, indicating a high degree of foam expansion.

Mechanical and Structural Insight Ashby Chart Classification: Mechanical testing revealed a low-modulus (0.12 – 0.2 MPa) and low-strength (0.59 MPa) behavior. When plotted on an Ashby chart, the material maps precisely into the polymeric foams quadrant, typical for highly porous, lightweight structures. Structure-Property Relationship: The final microstructure dictates the end-use. Flexible foams tolerate open cells to ensure breathability and elasticity, whereas rigid foams require small, closed cells to maximize thermal insulation and surface durability.

Bibliography

[1] Mubofu, E. B. Castor oil as a potential renewable resource for the production of functional materials. *Sustainable Chemical Processes* **2016**, *4*, 11.

[2] Shah, M.; Dai, J.-J.; Guo, Q.-X.; others Products and production routes for the catalytic conversion of seed oil into fuel and chemicals: a comprehensive review. *Science China Chemistry* **2015**, *58*, 1110–1121.

[3] Sharmin, E.; Zafar, F. *Flame Retardants*; IntechOpen, 2019.

[4] Wool, R. P. *Bio-Based Polymers and Composites*; Elsevier, 2005; p 1.

[5] QYResearch *Global Plastics Market Research Report 2026*; 2026.

[6] Global Information, Inc. *Plastics Market Size, Share, Growth and Global Industry Analysis*; 2025.

[7] Thomas, M. K 2025: European plastics in crisis. *Chemical Week* **2025**,

[8] Research and Markets *Polyurethane Global Market Report 2025*; 2025.

[9] 6Wresearch *Global Polyurethanes Market (2025 - 2031)*; 2025.

[10] Das, P.; others Biorefinery-based production of biodegradable bioplastics: advances and challenges in circular bioeconomy. *npj Materials Sustainability* **2025**, *3*, 42.

[11] Agbogo, V. U.; others Next-generation biodegradable polymers: toward a circular plastics economy. *AIMS Bioengineering* **2025**, *12*, 473–502.

[12] Kwon, S.; others Synthesis of rigid polyurethane foam from bio-based polyol obtained from microwave-assisted depolymerization of corn cob waste. *RSC Advances* **2025**, *15*, 18158–18172.

[13] Song, K.; others Synthesis, Modification and Prospect of Bio-based Polyurethane. *Leather Science and Engineering* **2025**, *35*, 48–53.

[14] Felekari, D. An overview of advances in methylene diphenyl diisocyanate (MDI) and toluene diisocyanate (TDI) based polyurethanes: Chemistry, properties, and applications. *Chemical Review and Letters* **2026**, *9*, 333–350.

[15] Suleman, S.; Khan, S. M.; Gull, N.; Aleem, W.; Shafiq, M.; Jamil, T. A Comprehensive Short Review on Polyurethane Foam. *International Journal of Innovation and Scientific Research* **2014**, *12*, 165–169.

[16] Ye, Y.; Zhu, Q. The development of polyurethane. *Materials Science: Materials Review* **2017**, *1*, 1–8.

[17] Ye, Y.; Zhu, Q. The development of polyurethane. *Materials Science: Materials Review* **2017**, *1*, 1–8, Department of Chemical Engineering, Beihai University of Technology.

[18] Akpan, U. G.; Jimoh, A.; Mohammed, A.; Mohammed, S. Preparation of Ricinoleic Acid from Castor Oil: A Review. *Journal of Chemical Engineering and Materials Science* **2021**, *12*, 12–21.

[19] Stöhr, T. Proteomic analysis of the endoplasmic reticulum of developing castor bean seeds- testing the feasibility of ER membrane topology elucidation using a sample of purified ER. M.Sc. thesis, Durham University, Durham, 2015.

[20] Mandal, Š. Physical and Chemical Properties of Selected Sample of Castor Oil, Ricinus communis L. *Kemija u industriji* **2023**, *72*, 187–192.

[21] Desroches, M.; Auvergne, R.; Boutevin, B.; others Synthesis of bio-based building blocks from vegetable oils: a platform chemicals approach. *Ocl* **2013**, *20*, 16–22.

[22] Jang, J. H.; Ha, J. H.; Kim, I.; Baik, J. H.; Hong, S. C. Facile Room-Temperature Preparation of Flexible Polyurethane Foams from Carbon Dioxide Based Poly(ether carbonate) Polyols with a Reduced Generation of Acetaldehyde. *ACS Omega* **2019**, *4*, 7944–7952.